UNIVERSIDADE FEDERAL DO RIO GRANDE DO SUL
INSTITUTO DE GEOCIÊNCIAS
PROGRAMA DE PÓS-GRADUAÇÃO EM GEOCIÊNCIAS

DIAGÊNESE METEÓRICA E RELACIONADA A DOMOS DE SAL EM RESERVATÓRIOS TURBIDITICOS TERCIÁRIOS DA BACIA DO ESPÍRITO SANTO, BRASIL

DANIEL MARTINS DE OLIVEIRA

ORIENTADOR – Prof. Dr. Luiz Fernando De Ros

Porto Alegre – 2018

DIAGÊNESE METEÓRICA E RELACIONADA A DOMOS DE SAL EM RESERVATÓRIOS TURBIDITICOS TERCIÁRIOS DA BACIA DO ESPÍRITO SANTO, BRASIL

DANIEL MARTINS DE OLIVEIRA

ORIENTADOR – Prof. Dr. Luiz Fernando De Ros

BANCA EXAMINADORA

Prof. Dr. Chang Hung Kiang – Departamento de Geologia Aplicada, Universidade Estadual Paulista Júlio de Mesquita Filho - UNESP

Prof. Dr. Almério Barros França – Programa de Pós-Graduação em Geologia, Universidade Federal do Paraná - UFPR

Profa. Dra. Karin Goldberg – Instituto de Geociências, Universidade Federal do Rio Grande do Sul - UFRGS

Dissertação de Mestrado apresentada como requisito parcial para obtenção do Título   de Mestre em Geociências

Porto Alegre – 2018

DEDICATÓRIA

Graças a De Ros.

AGRADECIMENTOS

Esta dissertação não seria possível sem o apoio de muitas pessoas.

Ao colega Marco Moraes, pela confiança e paciência.

À Petrobras, pelo suporte e financiamento.

Aos colegas Rute Morais, Fernando Taboada, Mathias Erdtmann, Luilson Tarcisio, Flávio Tschiedel, Rosilene Lamounier e Juliana Strim pelo auxílio direto com orientações, pela cessão de amostras e liberação de dados para incluir na dissertação e no artigo.

À minha gerente e colega Helga, pelo apoio e concessão de tempo para terminar essa dissertação.

Aos colegas Ailton e Camila pelo suporte com os dados de MEV e DRx.

Gratidão a De Ros, pela imensa generosidade e paciência.

RESUMO

A evolução diagenética de dois reservatórios turbidíticos terciários da porção *offshore* da Bacia do Espírito Santo, foi influenciada tanto por processos meteóricos como por processos relacionados a domos salinos adjacentes aos reservatórios, que tiveram diferente impacto sobre sua qualidade. A precipitação de pirita framboidal, dolomita microcristalina e siderita ocorreram sob condições eodiagenéticas marinhas. A percolação por água meteórica ocorreu ainda durante a eodiagênese, e promoveu extensiva caulinização ($\delta^{18}O_{SMOW}$=+15.3‰ a +18.2‰; δD_{SMOW}=-51‰ a -66‰) e dissolução de feldspatos, micas e intraclastos lamosos. Durante o progressivo soterramento da sequência (profundidades atuais: 2600-3000m) e consequente compactação, fluidos oriundos dos lutitos circundantes, modificados por reações com a matéria orgânica e carbonatos, deslocaram gradualmente os fluidos salobros marinhos-meteóricos, levando à precipitação de calcita poiquilotópica (valores médios: $\delta^{18}O_{VPDB}$= -6.6‰; $\delta^{13}C_{VPDB}$= -1.2‰). A composição dos fluidos mesodiagenéticos foi progressivamente modificada pela proximidade dos domos de sal, promovendo ubíqua albitização dos feldspatos e precipitação localizada de quartzo, calcita (valores médios: $\delta^{18}O$= -10.2‰; $\delta^{13}C$= -3.9‰) e dolomita em sela (valores médios: $\delta^{18}O$= -10.2‰; $\delta^{13}C$= -4.2‰). A análise de inclusões fluidas nos crescimentos de quartzo indicou que os fluidos precipitantes tinham salinidade predominantemente entre 9 e 13 % de NaCl (em peso) e temperaturas de homogeneização na faixa de 105^0 a 145^0 C. Estes valores são mais altos do que aqueles esperados para o gradiente geotérmico normal da área. A distribuição da albitização dos feldspatos sugere que as fraturas ao longo das margens dos domos de sal atuaram como caminho preferencial para a circulação das salmouras quentes. Os valores de $\delta^{13}C$ e $\delta^{18}O$ dos cimentos de calcita e dolomita seguem um padrão de covariância, mostrando um declínio desde daqueles representativos da água do mar (~0%), para $\delta^{13}C$ =-5.9‰ e $\delta^{18}O$ = -10.9‰ para a calcita, e $\delta^{13}C$ = -5.4‰ e $\delta^{18}O$ = -11.7‰ para a dolomita, o que sugere a progressiva participação da descarboxilação térmica da matéria orgânica dos lutitos com o soterramento. A compactação mecânica foi mais importante do que a cimentação na redução da porosidade, e a dissolução de feldspatos foi o processo mais importante na geração de porosidade nos reservatórios. Apesar da proximidade dos domos de sal, a intensidade dos processos diagenéticos foi moderada, já que não ocorreu autigênese de ilita, e a cimentação de quartzo foi limitada. Estas características podem estar relacionadas com o soterramento relativamente recente destes reservatórios. Este estudo mostra que a predição da diagênese e qualidade de reservatórios relacionados a domos de sal é uma função de múltiplas variáveis, incluindo as dimensões dos domos, o regime térmico regional da bacia, a condutividade térmica e de fluidos, e a composição mineral e propriedades geomecânicas dos reservatórios e litologias associadas.

Palavras-chave: diagênese, arenitos-reservatório, domos de sal, cinética.

ABSTRACT

The diagenetic evolution of two tertiary turbidite reservoirs from the offshore portion of the Espírito Santo Basin, eastern Brazil, was influenced by meteoric and salt dome-related processes, which had different impact on their quality. Marine eogenetic processes included the precipitation of framboidal pyrite, microcrystalline dolomite and siderite. Meteoric water influx during eodiagenesis occurred in response to relative sea-level falls that promoted extensive kaolinization ($\delta^{18}O$=+15.3‰ to +18.2‰; δD= -51‰ to -66‰) and dissolution of framework silicate grains. During progressive burial (present depths – 2600 m – 3000 m), connate marine fluids modified by reactions with organic matter and carbonates presented in the surrounding mudrocks gradually displaced brackish fluids generated by the meteoric influx and led to concretionary cementation by poikilotopic calcite (average $\delta^{18}O$= -6.6‰; $\delta^{13}C$= -1.2‰). Mesogenetic fluids were progressively modified by the proximity of salt domes, which led to ubiquitous feldspar albitization and localized quartz, calcite (average $\delta^{18}O$= -10.2‰; $\delta^{13}C$= -3.9‰) and saddle dolomite precipitation (average $\delta^{18}O$= -10.2‰; $\delta^{13}C$= -4.2‰). Fluid inclusion analysis in quartz overgrowths indicate that the precipitating fluids had salinities predominantly in the range 9-13 wt% NaCl equivalent and temperatures largely in the 105 – 145°C range. These values are higher than those expected considering the normal geothermal gradient for the area. The distribution of feldspar albitization suggests that the fracture systems along the salt domes margins acted as preferential pathways for such hot, saline diagenetic fluids. Isotopic values for calcite and dolomite cements follow a co-variance trend of decreasing $\delta^{13}C$ and $\delta^{18}O$ from close to marine (~0‰) towards negative values ($\delta^{13}C$ and $\delta^{18}O$ down to -5.9‰ and -10.9‰ for calcite; -5.4‰ and -11.7‰ for dolomite), suggesting increasing contribution from thermal decarboxylation with increasing temperature and depth. Mechanical compaction was more important than cementation in reducing depositional porosity, and the dissolution of framework silicate grains is the most important processes for enhancing reservoir quality. Despite the proximity to the salt domes, the intensity of the influenced diagenetic processes is relatively mild, as illite authigenesis is lacking, and quartz cementation is limited, features that may be related to the recent burial of the reservoirs.

Key words: meteoric incursion; salt dome-related diagenesis; thermobaric regime; kinetic constraints; turbidite reservoirs.

SUMÁRIO

Sobre a Estrutura desta Dissertação:

Esta dissertação de mestrado está estruturada em forma de artigo submetido e/ou aceito e/ou publicado em periódico classificado nos estratos Qualis-CAPES GEOCIÊNCIAS A1, A2, B1 ou B2. A sua organização compreende as seguintes partes principais:

PARTE I:

Introdução sobre o tema e descrição do objeto da pesquisa de Mestrado, onde estão sumarizados os objetivos e a filosofia de pesquisa desenvolvidos, o estado da arte sobre o tema de pesquisa, seguidos de uma discussão integradora contendo os principais resultados e interpretações deles derivadas.

PARTE II:

Corpo principal da dissertação, constituído por artigo científico, submetido ao periódico *Journal of Sedimentary Research*, precedido pela carta de aceite ou de recebimento do Editor do periódico.

1. INTRODUÇÃO

O entendimento da distribuição dos processos e produtos diagenéticos é de grande importância para uma caracterização apropriada da heterogeneidade e da qualidade de reservatórios clásticos (Morad *et al.* 2000; Morad *et al.* 2010). Isso é, entretanto, uma tarefa bastante complexa, já que a diagênese é governada por inúmeros parâmetros, tais como composição detrítica, fácies deposicional, condições climáticas, contexto tectônico e história de soterramento, que por sua vez controlam a composição química dos fluidos e os padrões de fluxo de fluidos (Wilson & Stanton, 1994; Morad *et al.* 2000).

No geral, a influência da diagênese nos reservatórios turbidíticos é relativamente pouco compreendida. Nas últimas décadas, a exploração de hidrocarbonetos foi progressivamente se concentrando em reservatórios arenosos turbidíticos depositados ao longo de margens continentais passivas. No Brasil, a despeito das novas descobertas dos depósitos "pré-sal", os reservatórios de turbiditos de água profunda ainda são grandes alvos exploratórios, já que correspondem à grande parte dos reservatórios e da produção de óleo.

Ao longo de décadas, um extenso banco de dados e uma ampla compreensão sobre a deposição dos reservatórios turbidíticos brasileiros foram gerados através de estudos sedimentológicos, estratigráficos e arquiteturais (Bruhn *et al.,* 2008; Fetter *et al.,* 2009; Empinotti *et al.,* 2011). Entretanto, com o avanço das atividades exploratórias, mais estudos sobre os controles diagenéticos sobre a qualidade dos reservatórios turbidíticos são requeridos, já que os reservatórios ainda a serem descobertos estão afetados por processos diagenéticos mais intensos e complexos.

No geral, acredita-se que a diagênese dos reservatórios turbidíticos seja mediada quase exclusivamente por fluidos marinhos (Bjorlykke & Aagard, 1992; Dutton, 2008). Nos últimos anos, entretanto, a influência da incursão de água meteórica na geração de alterações diagenéticas, portanto na qualidade de alguns reservatórios turbidíticos, têm sido ressaltados (Mansurbeg *et al.*, 2006; Prochnow *et al.*, 2006; Mansurbeg *et al.*, 2012). Por outro lado, a influência de domos de sal nos processos diagenéticos tem sido reconhecida a mais tempo em diversas sucessões sedimentares (McManus & Hanor, 1988, 1993; Posey & Kyle, 1988; Posey *et al.*, 1994; Esch & Hanor, 1995; Enos & Kyle, 2002; Bruno & Hanor, 2003; Archer *et al.*, 2004).

O objetivo deste trabalho é analisar a diagênese de dois reservatórios turbidíticos do Eoceno e Oligoceno, adjacentes a domos salinos, influenciados pela incursão de fluidos meteóricos e salmouras aquecidas, discutindo os controles e processos atuantes durante a sua evolução e seu impacto na qualidade destes reservatórios.

2. CONTEXTO GEOLÓGICO

A Bacia do Espírito Santo, a leste da margem continental brasileira, foi formada durante o Eocretáceo com a fragmentação neocomiana do supercontinente Gondwana, e desenvolvida durante a subsequente abertura do oceano Atlântico Sul, que resultou na separação e deriva dos continentes sul-americano e africano. A Bacia do Espírito Santo compreende uma área de aproximadamente 25.000 Km², sendo limitada a leste pelo complexo vulcânico de Abrolhos e a oeste pelo embasamento cristalino pré-cambriano. Este último é constituído por migmatitos, granulitos, gneisses e granitos, e ocorre como blocos falhados homoclinais inclinados em direção a leste (Fig.1) (Del Rey & Zembruscky, 1991).

As principais rochas geradoras na bacia são de idade neocomiana, sendo folhelhos lacustres da fase rifte pertencentes à base da Fm. Cricaré (Estrella *et al*., 1984; Carvalho, 1989). Estes folhelhos são sucedidos por conglomerados e arenitos de idade aptiana da Fm. Mariricu, intercalados com pelitos, calcários e anidritas, que representam rápidos eventos de afogamento na bacia. Após a deposição desta formação, uma incursão marinha sob condições de circulação restrita e clima árido precipitou uma espessa sequência de evaporitos aptianos (Membro Itaúnas). Carbonatos marinhos de plataforma rasa (Membro Regência) e depósitos clásticos de *fan-delta* (Membro São Mateus) da Fm. Barra Nova foram depositados durante o Albiano e o Cenomaniano.

Durante o Neocretáceo e o início do Terciário, a bacia foi submetida à subsidência térmica e a flexura crustal que geraram o basculamento de blocos em direção à leste e, juntamente com a halocinese associada, controlaram a deposição de uma espessa sequência de areias turbidíticas e lamas marinhas da Fm. Urucutuca (Fig. 1). Na parte mais ao norte da bacia, um vulcanismo intraplaca, de caráter básico alcalino, teve início no final do Neocretáceo com seu pico de atividade durante o Eoceno (37 Ma; Cordani & Blazekovic, 1970), e originou a grande plataforma vulcânica de Abrolhos.

A área estudada compreende dois campos de gás e óleo, denominados Cangoá e Peroá, com reservatórios respectivamente de idade eocênica e oligocênica, ambos

localizados na chamada "província dos domos de sal" (distantes em torno de 40 Km da costa) na parte sul da bacia (Fig. 2). A deposição dos turbiditos da Fm. Urucutuca na área ocorreu dominantemente como complexo de corpos arenosos canalizados e diques marginais, intercalados com lamitos hemipelágicos, depositados na base do talude, ao longo de depressões originadas pelo diapirismo do sal aptiano.
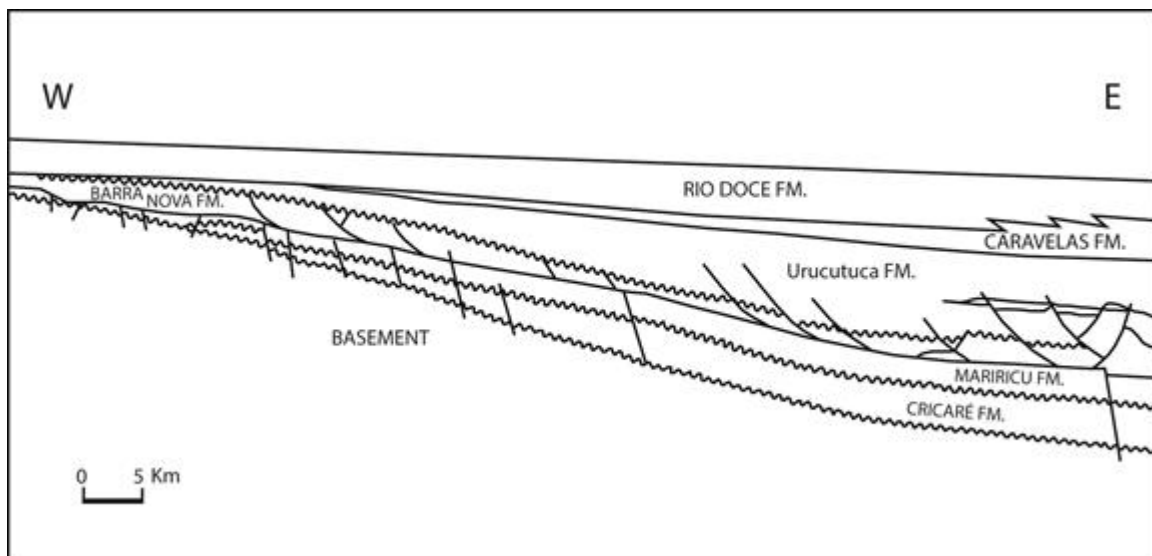
Figura 1. Seção esquemática longitudinal da bacia mostrando o espessamento da Formação Urucutuca em direção a leste (modificado de Del Rey & Zembruscky, 1991)

Apesar da diferença de idade, os intervalos turbidíticos de Cangoá e Peroá foram depositados dentro de um ciclo completo de rebaixamento e elevação do nível relativo do mar, sendo limitados por discordâncias regionais. Quedas no nível de base levaram ao transporte de areias através da plataforma continental para partes mais profundas da bacia.
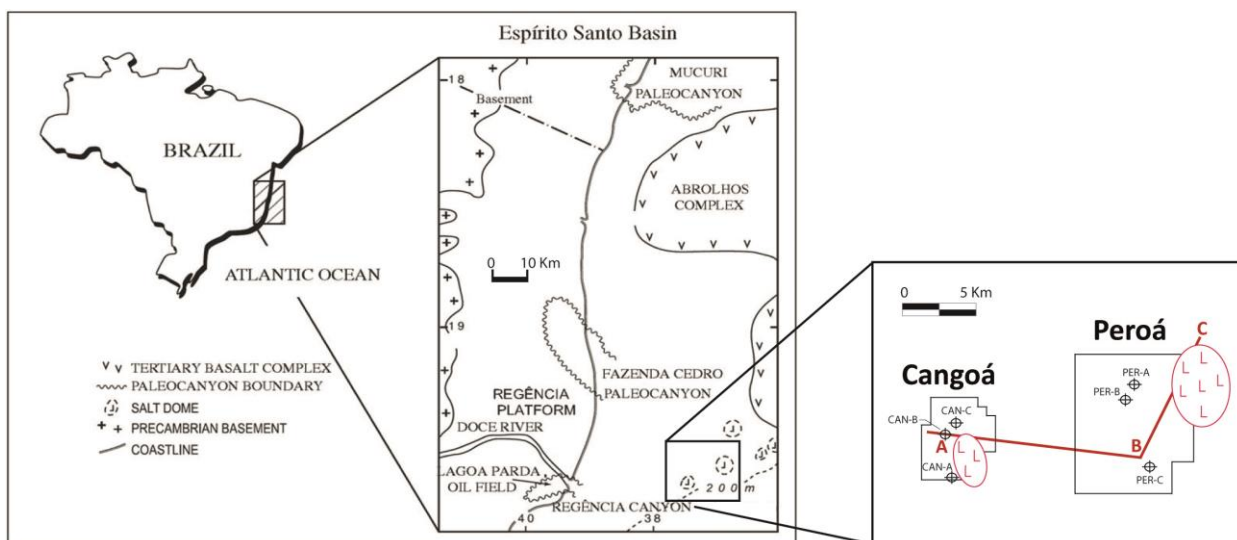
Figura 2. Mapa de localização da área estudada com indicação dos dois campos em detalhe, poços estudados e localização dos domos de sal. Figura apresentando contexto geral retirada de Mansurberg *et al.* (2012).

2.1. Contexto Tectônico e Diapirismo de Sal

Uma parte da porção sul da Bacia do Espírito Santo é conhecida como "província dos domos de sal" por conter estruturas provenientes da deformação dos evaporitos aptianos e pela sua intrusão ativa em rochas mais novas a eles sobrepostas. Onde a carga da pilha sedimentar sobre sequências evaporíticas não é uniforme, o sal pode fluir para áreas de mais baixa pressão, formando almofadas e domos, que podem evoluir posteriormente para estruturas diapíricas.

A halocinese, iniciada no Albiano, ocorreu devido ao basculamento da bacia e à implantação e progradação de uma plataforma mista (carbonatos e arenitos), e atuou pelo menos até o eoceno, tendo sido um processo importante na distribuição, acumulação e evolução diagenética das areias turbidíticas nas áreas de Cangoá e Peroá.

5

O campo de Cangoá está localizado no flanco noroeste de um dos domos de sal da província. Nas imagens sísmicas em planta ("time slice"), é possível identificar em torno da estrutura, um sistema de falhas e fraturas concêntricas que afetaram os arenitos e lutitos circundantes. O domo de sal serviu como barreira para a acumulação das areias, o que é evidenciado pelo progressivo adelgaçamento das camadas em sua proximidade. Sua contínua movimentação provocou o soerguimento de parte das camadas arenosas que preenchem a calha neo-eocênica e condicionou também o fraturamento de grãos e os estágios iniciais da evolução diagenética dos reservatórios.

O Campo de Peroá situa-se em um contexto estrutural bastante particular em relação às demais acumulações conhecidas na Bacia do Espírito Santo. A halocinese atuou principalmente na distribuição dos reservatórios, tendo sido pouco importante em sua estruturação. Neste caso, é muito provável que a movimentação do domo tenha antecedido a deposição dos arenitos oligocênicos de Peroá. Além disso, estes reservatórios estão mais afastados do domo de sal associado do que os reservatórios de Cangoá. A estruturação deste campo está mais relacionada a mecanismos de compactação diferencial dos reservatórios e dos lutitos adjacentes sobre um alto estrutural de origem compressiva (VIEIRA *et al.*, 1999). Essa grande estrutura, anteriormente interpretada como um domo salino revelou-se, após a perfuração, uma cunha constituída predominantemente por um espesso intervalo de lutitos cretácicos. Essa descoberta motivou a discussão sobre o papel do diapirismo do sal como causa ou mesmo um subproduto de uma tectônica compressiva mais regional. O fato da movimentação e intrusão do sal não ser competente para gerar estruturas em espessos pacotes de lutitos, como observado no Campo de Peroá, com significativo grau de litificação favorece a última hipótese.

3. ASPECTOS CONCEITUAIS

Do ponto de vista geoquímico, a diagênese compreende um campo de condições físicas e químicas que controla os processos geológicos atuantes sobre todos os tipos de materiais na superfície da crosta terrestre, nos primeiros milhares de metros de profundidade (antecedendo o campo do metamorfismo). Estes processos são controlados pela pressão, temperatura, composição dos fluidos intersticiais e pela composição química e mineralógica dos materiais. Os processos diagenéticos influenciam diretamente a qualidade dos reservatórios de hidrocarbonetos e atuam de maneira positiva, preservando e gerando porosidade, ou negativa, reduzindo ou destruindo totalmente a porosidade.

3.1. Estágios da diagênese

A partir das definições originais de Choquette & Pray (1970) e de Schmidt & McDonald (1979), os estágios da diagênese clástica foram redefinidos por Morad *et al.* (2000), que atribuíram intervalos de profundidade e temperatura para os conjuntos dos principais processos relacionados a cada uma das zonas. Sua distribuição espacial pode ser encontrada na Figura 3.

Eodiagênese: atuante desde a superfície até profundidades em torno de 2 Km, até cerca de 70^0C de temperatura, sob baixas pressões, e tempo de residência muito variável. É influenciada pela dinâmica e composição dos fluidos deposicionais e/ou pela circulação de água superficial (marinha/meteórica).

Mesodiagênese rasa: considerada neste trabalho como Mesodiagênese compactacional, é atuante em profundidades que variam de 2 a 3 Km, com temperaturas entre 70 e 100^0C, em condições de pressão e temperaturas crescentes, sob ação de fluidos diagenéticos progressivamente modificados pelas reações com os minerais e influenciados pela interação com fluidos conatos provenientes de lutitos, circulando principalmente por compactação.

Mesodiagênese profunda: considerada neste trabalho como Mesodiagênese termobárica. Profundidades são superiores a 3 Km e temperaturas maiores que 100^0C. Expulsão de água estrutural dos argilominerais; exportação e importação de solutos a partir das reações de ilitização e decomposição térmica das esmectitas. A evolução da

mesodiagênese pode dar-se por soerguimento, para a telodiagênese, ou por soterramento crescente para o metamorfismo, através da transição denominada anquimetamorfismo.
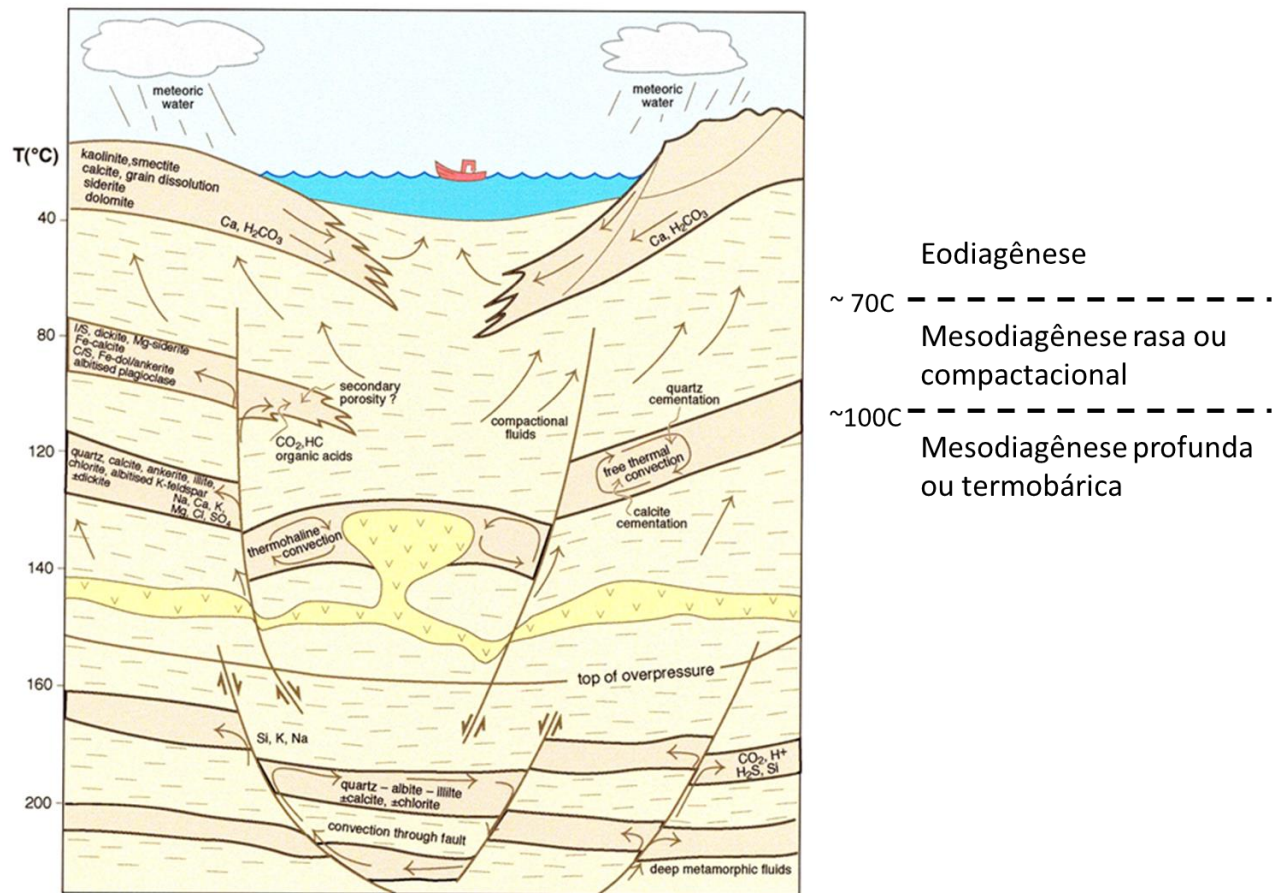
Figura 3. Distribuição espacial e temporal das alterações diagenéticas e dos padrões de fluxo de fluidos e transporte de massa em uma bacia hipotética (Morad *et al.*, 2000).

Telodiagênese: desenvolvida através da re-exposição às condições superficiais de rochas previamente soterradas por soerguimento e erosão de parte da seção, ou da infiltração de água meteórica a grandes profundidades.

3.2. Principais processos diagenéticos

Os principais processos diagenéticos podem ser sumarizados como segue:

Compactação: ocasionada pelo soterramento, com redução do espaço poroso intersticial. Pode ser física, através do rearranjo, fraturamento ou esmagamento dos grãos, ou química, através da dissolução por pressão nos contatos intergranulares ou ao longo de estilolitos.

Dissolução: pode afetar constituintes primários ou diagenéticos. Pode ser congruente, total, com total remoção dos materiais como íons em solução (ex: em carbonatos); ou incongruente, incompleta, com manutenção de parte dos íons na forma de novos minerais (ex: feldspatos → caulinita).

Autigênese: precipitação de novos minerais, cimentando os poros intergranulares ou substituindo espacialmente constituintes pré-existentes via dissolução e precipitação.

Hidratação / desidratação: entrada ou saída de água da estrutura cristalina (ex: anidrita ←→ gipsita).

Oxidação: perda de elétrons em alguns materiais (chamados doadores), na superfície ou próximo a ela, sob influência de O_2 ou bactérias aeróbicas; ex: Fe^{2+}→ Fe^{3+}, formando hematita.

Redução: ganho de elétrons em alguns materiais (chamados aceptores), sob influência da matéria orgânica e de bactérias anaeróbicas; ex: Fe^{3+} → Fe^{2+}, formando pirita, siderita.

Recristalização: Crescimento ou diminuição do tamanho cristalino, mantendo-se a mesma composição mineralógica.

Estabilização/ neomorfismo / inversão: substituição de uma fase mineralógica por outra de composição similar; ex: aragonita → calcita.

3.3. Controles da diagênese clástica

Os principais controles atuantes sobre a diagênese são a composição detrítica, a composição dos fluidos intersticiais, o fluxo dos fluidos e fatores físicos como pressão, temperatura e tempo (Morad *et al.*, 2012) (Fig. 4). A composição detrítica é definida em função essencialmente da proveniência, controlada pelas rochas-fonte, pela geografia e pelo clima. A composição dos fluidos é controlada inicialmente pelo ambiente de deposição. Este último controla também a textura, estrutura e geometria dos sedimentos e, portanto as características petrofísicas que condicionarão em parte a evolução do fluxo de fluidos. Os fluidos circulando pelos arenitos são comumente modificados pela interação com evaporitos e lutitos durante o soterramento. A composição dos constituintes diagenéticos anteriormente formados influencia as reações diagenéticas durante o soterramento ou soerguimento posteriores. A temperatura, pressão e tempo são parâmetros controlados pela história de soterramento e térmica, em função do ambiente tectônico da sucessão sedimentar.
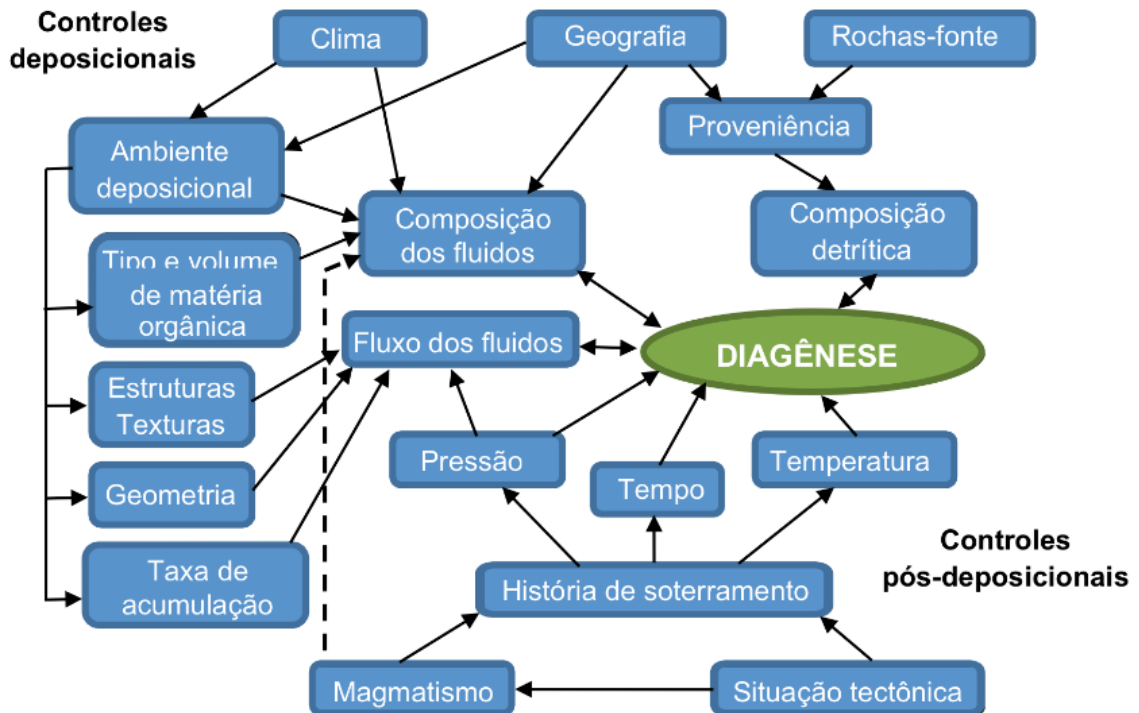
Figura 4. Representação das relações entre os parâmetros controladores da diagênese (modificado de Morad *et al.*, 2012).

4. EODIAGÊNESE METEÓRICA EM DEPÓSITOS TURBIDÍTICOS

A distribuição espacial das alterações diagenéticas em sedimentos marinhos e transicionais é fortemente influenciada pelas variações no nível do mar, distribuição das fácies deposicionais e a extensão de mistura entre águas meteóricas e marinhas. As condições climáticas, permeabilidade dos sedimentos e a disponibilidade de uma cabeceira hidráulica eficiente controlam a magnitude das alterações induzidas pela incursão de fluidos meteóricos através dos sedimentos transicionais e marinhos abaixo do substrato. A profundidade máxima de incursão de água meteórica na bacia marinha é limitada pela pressão dos fluidos ascendentes compactacionais, que por sua vez, é condicionada pela taxa de subsidência e sedimentação da bacia (Figura 5). Devido a isso, as condições ideais para a incursão meteórica ocorrem comumente na telodiagênese, porque durante a eodiagênese os sedimentos depositados na bacia estão submetidos à compactação e a entrada do fluido meteórico compete com o fluido compactacional ascendente.
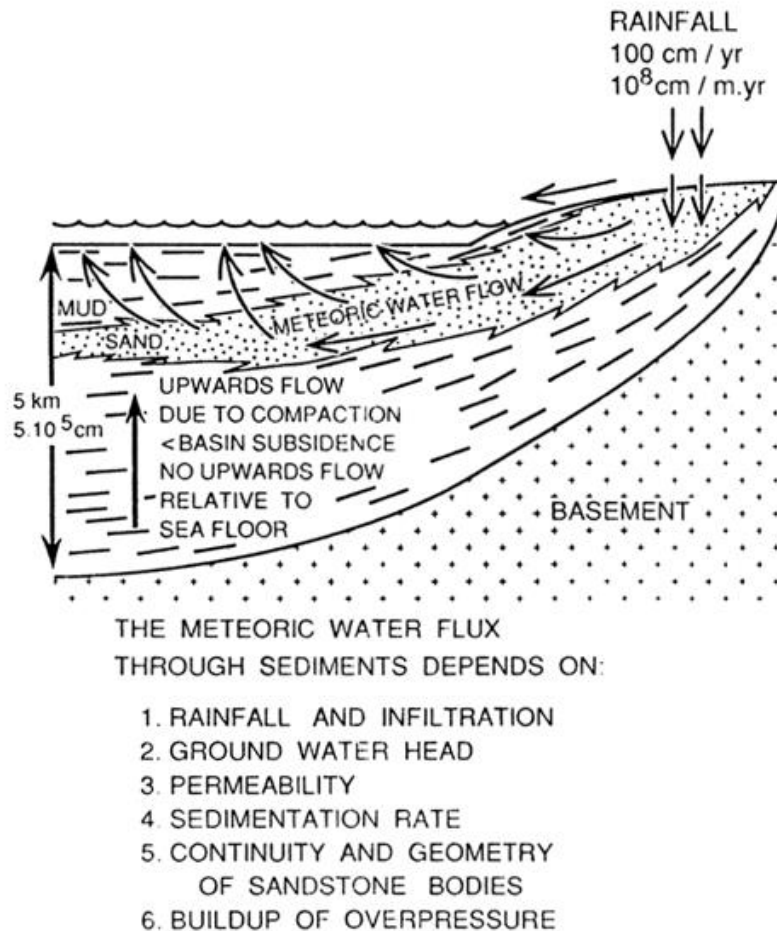
Figura 5. Principais fatores de controle da incursão de fluidos meteóricos em uma bacia marinha. (MORAD *et al.*, 2012).

Um número crescente de comunicações científicas demonstra que a incursão de fluidos meteóricos também ocorre em arenitos de água profunda, como nos turbiditos do Cretáceo e do Terciário das bacias de Shetland e marginais do Brasil (Hayes & Boles, 1992; Carvalho *et al.*, 1995; Mansurbeg *et al.*, 2006, 2008; Prochnow *et al.*, 2006). Em determinadas condições, as zonas meteóricas e de mistura entre fluidos marinhos e meteóricos migram em direção à bacia e induzem a alterações diagenéticas mesmo em sedimentos marinhos profundos. A percolação ativa de fluidos insaturados meteóricos causa a dissolução de silicatos detríticos (principalmente feldspato e micas) e a precipitação de caulinita autigênica.

No contexto de água profunda, a distribuição espacial da caulinita e da dissolução de grãos são influenciadas pela quantidade e distribuição de silicatos detríticos instáveis, pela permeabilidade dos litotipos, precipitação meteórica anual, e pela razão do fluxo de fluidos e condutividade hidráulica dos corpos arenosos, sendo mais pronunciadas em corpos lateralmente persistentes e permeáveis, como depósitos amalgamados em canais

turbidíticos, e menos importantes em sedimentos mais finos, como depósitos de *levee* e de franjas de lobos distais.

Localmente, falhas conectadas aos corpos arenosos ou a importantes superfícies de descontinuidade, como discordâncias regionais, podem desempenhar um importante papel como condutos de ligação (Ketzer *et al.*, 2003).

Durante regressões forçadas e períodos de nível baixo do mar, extensas áreas são expostas na plataforma, levando a um alargamento das áreas de recarga meteórica. A percolação de água meteórica não resulta somente na dissolução e caulinização de grãos silicáticos, mas também, em alguns casos, na precipitação de cimentos precoces carbonáticos a partir de sua mistura com o fluido marinho (Rossi, Cañaveras, 1999). Caracteristicamente, cimentos carbonáticos que precipitaram durante uma regressão apresentam um decréscimo no conteúdo de Sr^{2+}, Na^+ e Mg^{2+}, tanto quanto valores mais baixos de $\delta^{18}O$ e mais altos de $^{87}Sr/^{86}Sr$ em direção ao centro dos poros, indicando uma progressiva modificação das águas de poro em direção a composição meteórica (Kaldi & Gidman, 1982; Glasmann *et al.*, 1989a; Hart *et al.*, 1992; Morad *et al.*, 1992).

Nos casos em que a carga de hidrocarbonetos antecedeu à incursão de fluidos meteóricos em bacias marinhas, esta, juntamente com a ação de bactérias, pode promover a degradação de óleo dentro dos reservatórios (Prochnow *et al.*, 2006). Óleos biodegradados são ricos em frações pesadas tais como resinas e asfaltenos, e têm viscosidade, acidez e conteúdo de enxofre mais altos (Wilhelms *et al.*, 2001). A deposição de asfaltenos em superfícies de grãos minerais pode influenciar a molhabilidade e a diagênese dos reservatórios (Ehrenberg *et al.*, 1995; Daughney, 2000; Barclay & Worden, 2000).

Desta maneira, o entendimento e predição temporal e espacial dos produtos diagenéticos relacionados à incursão de fluidos meteóricos em uma bacia são importantes tanto para as atividades de exploração quanto de produção.

5. MESODIAGÊNESE TERMOBÁRICA: INFLUÊNCIA DE DOMOS SALINOS NA DIAGÊNESE

5.1. Padrões térmicos e fluxo de fluidos próximos a domos de sal

A literatura sobre os efeitos da alta condutividade térmica dos domos de sal na circulação do calor e dos fluidos dentro das bacias sedimentares é vasta. As áreas sobre e em torno de domos de sal são conhecidas por experimentar significativas anomalias térmicas, que podem promover, dentre outros efeitos, maturação diferencial da matéria orgânica (Rashid, 1978; O'Brian & Lerche, 1987). Outro efeito conhecido relacionado aos abruptos gradientes térmicos em tornos dos domos de sal envolve a convecção de fluidos, devida à menor densidade dos fluidos aquecidos ao longo dos flancos dos domos em relação aos fluidos acima e em torno da parte superior destas estruturas (convecção livre do tipo Rayleigh-Bénard; cf. Ranganathan; Hanor, 1988; Evans *et al.*, 1991). Este mecanismo é normalmente amplificado pela dissolução do sal a partir dos domos pelos fluidos ascendentes, progressivamente mais densos à medida que se resfriam, que submergem longe das estruturas para serem novamente aquecidos e re-circulados. Esse mecanismo é conhecido como convecção termohalina (Hanor, 1987a; Evans & Nunn, 1989; Evans *et al.*, 1991; Mcmanus & Hanor, 1993; Sharp e*t al.*, 2001).

A dissolução do sal por tais sistemas de convecção é considerada como o controle dos padrões de salinidade observados em extensas áreas do golfo do México e em outras bacias (e.g. Hanor, 1987b, 1994; Mcmanus & Hanor, 1993; Sharp *et al.*, 2001).

Os fluidos convectivos promovem uma série de interações com as rochas circundantes ou capeadoras aos domos (Posey & Kyle, 1988; Light & Posey, 1992), incluindo mineralizações (*e.g.* Ulrich *et al.*, 1984; Charef & Sheppard, 1991; Posey *et al.* 1994; Kyle & Saunders, 1997), e redução da qualidade de reservatórios clásticos (*e.g.* MCMANUS & Hanor, 1988; Burley, 1993; Enos & Kyle, 2002; Archer *et al.*, 2004) e carbonáticos (*e.g.* Jensenius & Munksgaard, 1989).

5.2. Evolução da diagênese e qualidade de reservatório de arenitos adjacentes a domos de sal

Com relação à evolução diagenética e da qualidade de reservatório de arenitos adjacentes a domos de sal, há dois aspectos a serem considerados.

O primeiro diz respeito aos tipos de processos e produtos diagenéticos causados pela amplificação térmica e do fluxo de fluidos, e ao impacto deles na porosidade e permeabilidade de reservatórios. O regime térmico mais pronunciado vai, consequentemente, aumentar a solubilidade do quartzo detrítico, aumentando assim a compactação química através da dissolução por pressão nos contatos intergranulares e em superfícies estilolíticas, bem como promover a cimentação por crescimentos de quartzo (cf. Giles *et al.*, 2000; Archer *et al.*, 2004). A circulação desses fluidos amplifica a cimentação de quartzo, fornecendo solutos e mantendo o suprimento de sílica para sustentar o processo.

Outros processos diagenéticos responsáveis pelo detrimento da porosidade de reservatórios próximos a domos de sal incluem cimentação carbonática e a precipitação de pirita e outros sulfetos substituindo e cimentando grãos (e.g., Mcmanus & Hanor, 1988; Enos & Kyle, 2002). Estes sulfetos são precipitados a partir do H_2S gerado pela redução térmica de sulfatos (Machel, 1987; 2001), provenientes da dissolução de evaporitos. Entretanto, o H_2S pode também contribuir para a geração de porosidade através da dissolução de grãos e cimentos (Surdam *et al.*, 1989; Burley, 1993). Outros processos diagenéticos importantes que podem ainda impactar a qualidade de reservatórios de arenitos próximos a domos de sal são a cimentação e a redução da permeabilidade por ilita fibrosa (e.g., Hancock, 1987; Glasmann *et al.*, 1989b; Bjorlykke & Aagaard, 1992), a cimentação por anidrita, barita, siderita-magnesita, até mesmo halita, promovida pela disponibilidade de K^+, SO_4^{2+}, Ba^{2+}, Mg^{2+} e Cl^- em solução, provenientes da dissolução de evaporitos.

A albitização de feldspatos detríticos controlada pelas altas atividades de Na^+ é também um processo comumente identificado em bacias influenciadas por evaporitos, mas tem normalmente pouco impacto na qualidade dos reservatórios, embora a grande quantidade de transferência de massa envolvida neste processo.

A implicação destes padrões para a exploração de hidrocarbonetos é clara, desde que a maioria dos processos diagenéticos promovidos pelo aumento do fluxo térmico e de

fluidos próximos aos domos de sal contribuem para a redução da qualidade de reservatórios. Entretanto, a área mais intensamente afetada será função de uma série de variáveis, como por exemplo, as dimensões do domo salino, o regime térmico regional da bacia, a condutividade térmica e dos fluidos, e a composição mineral dos reservatórios e litologias associadas.

6. AMOSTRAS E MÉTODOS ANALÍTICOS

Ao todo, foram selecionadas para este estudo 150 amostras oriundas de oito poços testemunhados (quatro poços no Campo de Cangoá e outros quatro no Campo de Peroá) no intervalo da Fm. Urucutuca.

As composições modais dos arenitos e as interpretações paragenéticas foram obtidas através de análise sistemática qualitativa e quantitativa das amostras através do sistema Petroledge©, pela contagem de 300 pontos em lâminas petrográficas com impregnação de resina epoxy azul. Com isso, foi possível reconstituir a composição e porosidade original e modificada dos arenitos analisados em relação a cada um dos estágios diagenéticos reconhecidos (eogenético marinho → eogenético meteórico → mesogenético compactacional → mesogenético termobárico). O tingimento com solução hidroclorídrica de Alizarina Red-S e ferrocianeto de potássio foi realizado com o objetivo de diferenciar calcitas e dolomitas (cf. Friedman, 1959). Análises de microscopia eletrônica de varredura no modo de elétrons secundários (BSE) foram realizadas para melhor definir as relações paragenéticas entre constituintes primários e diagenéticos em lâminas delgadas selecionadas utilizando um microscópio JEOL JSM-6690LV equipado com espectrômetro de energia dispersiva (EDS) para identificação da composição elementar dos constituintes.

Para a identificação dos argilominerais presentes nos arenitos e lutitos, análises de DRx em frações selecionadas de 2µm foram realizadas em 69 amostra orientadas, utilizando um difratômetro Rigaku D/MAX – 2200/PC sob as seguintes condições: 40 mA e 40 kV, com abertura de 2, 0,3 e 0,6 mm. As amostras foram secas ao ar, saturadas com etileno-glicol e aquecidas à 490°C por 4 horas.

Análises geoquímicas de isótopos estáveis de carbono e oxigênio foram conduzidas no "Laboratory for Isotopic Studies", da Universidade de Windsor, em 17 amostras de arenitos com cimentação carbonática. A extração do CO_2 liberado da calcita e da dolomita a partir

das amostras foi realizada seguindo o método de separação química de Al-Aasm *et al.* (1990). Para isso, as amostras foram reagidas no vácuo com ácido fosfórico concentrado à 100% durante 1 hora a 25°C e para a calcita e por 24 horas a 50°C para a dolomita. Então, o gás CO_2 extraído foi analisado em um espectrômetro de massa Delta Plus para o cálculo das razões isotópicas. Os fatores de fracionamento utilizados na reação com o ácido fosfórico foram 1,01025 para a calcita (Friedman & O'Neil, 1977) e 1,01060 para a dolomita (Rosenbaum & Sheppard, 1986). Os valores de delta (δ) para oxigênio e carbono são reportados em per mil (‰) relativos ao padrão "Vienna Pee Dee Belemnite" (VPDB). O erro de precisão das análises ficou em torno de 0,05‰, tanto para carbono como para oxigênio.

Análises isotópicas de oxigênio e hidrogênio em caulinitas em sete amostras foram conduzidas no "Laboratory for Stable Isotope Science" da Universidade de Western Ontario, e os resultados são reportados em per mil (‰) em relação ao padrão "Vienna Standard Mean Ocean Water" (V-SMOW). As amostras foram pulverizadas e separadas em diferentes frações granulométricas e analisadas para difratometria de raios-X (DRX), com o objetivo de identificar a fração mais adequada para a análise isotópica, sendo aquela com maior quantidade de caulinita e menor contaminação de micas. A fração escolhida foi aquecida e bombeada em recipientes para a reação com Ni sob vácuo à 300°C por duas horas antes da reação com ClF_3. As amostras então foram reagidas à 580°C durante uma noite. O oxigênio foi extraído dos silicatos utilizando o método de Clayton & Mayeda (1963), modificado para a utilização de trifluoreto de cloro (ClF_3) e convertido quantitativamente para CO_2 sobre grafite ultra aquecido. As amostras foram analisadas em dois espectrômetros de massa (Optima e Prism) utilizando o padrão NBS-28 para calibração dos padrões para quartzo e argilominerais do laboratório. A reprodutibilidade das amostras foi melhor que +0,3 per mil, no geral. O hidrogênio foi extraído da caulinita seguindo o procedimento de Bigeleisen *et al.* (1952), modificado por Vennemann & O'Neil (1993). Primeiramente, as amostras foram secas durante uma noite à 105°C em regime de vácuo, e então aquecidas a 1200°C utilizando uma tocha de oxigênio-propano. Os grupos de hidroxila foram convertidos à H_2O pela reação com óxido de cobre a 400-600°C, e então as moléculas de H_2O foram reduzidas para o gás H_2 sobre placa de Cr à 900°C. As composições isotópicas de hidrogênio foram medidas utilizando espectrômetro de massa VG-Prism-II calibrado para VSMOW e SLAP (Standard Light Antarctic Precipitation) comparando com quatro padrões do laboratório. A reprodutibilidade das amostras é comumente melhor que ±5 per mil.

Cinco amostras foram selecionadas para a análise de inclusões fluidas (microtermometria) objetivando a determinação da temperatura de homogeneização e salinidade das inclusões aquosas presentes nos cimentos de quartzo. As análises foram realizadas pela empresa Fluid Inc. – FIT Technologies, utilizando microscópio petrográfico convencional equipado para luz branca transmitida e ultravioleta, acoplado de uma platina modificada de aquecimento e resfriamento projetado pela própria empresa. Isso permite que as amostras possam ser aquecidas até 700°C, com a passagem de ar ou nitrogênio quente, ou resfriada até -190°C, com a passagem de gás nitrogênio resfriado por nitrogênio líquido. Os conjuntos de inclusões inicialmente foram diferenciados em função da sua relação com o mineral hospedeiro e a consistência de parâmetros visuais (*e.g.* razão aparente líquido/vapor). As inclusões foram selecionadas para quantificação tendo base essa primeira triagem.

7. RESULTADOS E INTERPRETAÇÕES

Os reservatórios turbidíticos estudados são arcósios e imaturos tanto textural- quanto composicionalmente e seus modos de composição detrítica indicam que a área-fonte destes sedimentos era caracterizada por terrenos do embasamento granítico-gnáissico que foram progressivamente soerguidos e constitui atualmente a Serra do Mar.

A deposição dos fluxos turbidíticos na área de Cangoá foi influenciada pela presença de um domo de sal que provavelmente atuou como barreira para os fluxos gravitacionais arenosos. A progressiva movimentação do diápiro, ainda em um regime de soterramento não efetivo, levou a um fraturamento irregular de grãos de quartzo e feldspatos, o que pode ter favorecido a circulação de fluidos e a posterior dissolução, caulinização e albitização dos grãos de feldspato. No campo de Peroá, a influência do domo de sal foi mais limitada e parece não ter exercido um controle tão forte durante a sua deposição como observado em Cangoá.

A evolução diagenética destes reservatórios foi inicialmente influenciada, durante a eodiagênese, por processos marinhos mediados por microorganismos, caracterizados pela autigênese de pirita, dolomita e siderita, e pela incursão de fluidos meteóricos, registrada pela dissolução e caulinização de grãos silicáticos. A intensa expansão das

lamelas de muscovita por caulinita e as razões isotópicas de $\delta^{18}O$ (+15.3‰ - +18.2‰) e δD (-51‰ - -66‰) obtidas nestas mesmas caulinitas corroboraram sua origem meteórica.

A percolação de fluidos meteóricos nestes reservatórios turbidíticos foi condicionada pela cabeceira hidráulica formada pelo soerguimento da área-fonte e pela expansão da área de recarga meteórica associada ao rebaixamento do nível do mar e a exposição de grande parte da plataforma continental à época. Com o progressivo soterramento, fluidos modificados pela interação com os domos de sal e lutitos circundantes interagiram com estes reservatórios e condicionaram a precipitação de quartzo, albita e carbonatos tardios. Dados de inclusões fluidas obtidos nos crescimentos de quartzo, em ambos os campos, documentam condições de mais alta temperatura e salinidade (9-13% em peso de NaCl e $Th= 105^0–145^0C$) durante a evolução destes reservatórios quando comparadas às suas atuais condições.

Apesar da proximidade dos reservatórios com os domos de sal e da sua exposição a mais altas temperaturas e salinidades, durante a mesodiagênese, a intensidade dos processos diagenéticos foi relativamente moderada. A ausência de ilita fibrosa e da cimentação limitada de quartzo nestes reservatórios apesar da disponibilidade de fontes internas e externas à sua precipitação, indicam a sua curta residência nestas condições de temperatura e o forte controle cinético destas reações. Mesmo instável acima de 100ºC, convertendo-se em 'quartzo + ilita', a assembleia mineral 'K-feldspato + caulinita' ainda está preservada nestes arenitos. E mesmo a incursão de salmouras ricas em K^+ a partir da dissolução dos domos de sal circundantes não foi condição suficiente para a cimentação de ilita neoformada nos arenitos. Entretanto, os intraclastos argilosos presentes nos arenitos e os lutitos intercalados na sequência estão ilitizados. Isso ocorre porque a reação de transformação de esmectita a ilita é distinta e condicionada por diferentes parâmetros termodinâmicos e cinéticos, sendo favorecida energeticamente, não requerendo temperaturas tão altas quanto a neoformação de ilita fibrosa.

O curto intervalo de tempo das condições de mais alta temperatura e salinidade está provavelmente relacionado ao comportamento intermitente das falhas como condutos efetivos para a migração de fluidos, tendo estado provavelmente inativas durante a maior parte da evolução dos reservatórios.

8. REFERÊNCIAS BIBLIOGRAFICAS

Al-Aasm, I.S., Taylor, B.E. & South, B., 1990. Stable isotope analysis of multiple carbonate samples using selective acid extraction. *Chemical Geology*, 80, 119-125.

Archer, S.G., Wycherley, H.L., Watt, G.R., Baron, M.L., Parnell, J. & Chen, H., 2004. Evidence for focused hot fluid flow within the Britannia field, offshore Scotland, UK: *Basin Research*, 16(3): 377-395.

Barclay, S.A. & Worden, R.H., 2000. Effects of reservoir wettability on quartz cementation in oil fields. *In*: Worden, R.H. & Morad, S., (Eds.). *Quartz Cementation in Sandstones*, International Association of Sedimentologists, Special Publication 29, Blackwell Science, Oxford, p. 103–117.

Bigeleisen, J., Perlman, M.L. & Prosser, H.C., 1952. Conversion of hydrogenic materials to hydrogen for stable isotopic analysis. *Analytical Chemistry*, 24: 1356-1357.

Bjørlykke, K., & Aagaard, P., 1992. Clay minerals in North Sea sandstones. *In:* Houseknecht, D.W. & Pittman, E.D., (Eds.). *Origin, Diagenesis, and Petrophysics of Clay Minerals in Sandstones*, SEPM Special Publication 47, p. 65-80.

Burley, S.D., 1993. Models of burial diagenesis for deep exploration plays in Jurassic fault traps of the Central and Northern North Sea. *In:* Parker, J.R., (Ed.). *Petroleum Geology of Northwest Europe*: Proceedings of the 4th Conference: London, UK, The Geological Society, p. 1353-1375.

Bruhn, C.H.L., 2001. Contrasting types of Oligocene/Miocene giant turbidite reservoirs from deep water Campos Basin, Brazil. *In*: AAPG Distinguished Lecture.

Bruno, R.S. & Hanor, J.S., 2003. Large-scale fluid migration driven by salt dissolution, Bay Marchand Dome, offshore Louisiana: *GCAGS Transactions*, v. 53, p. 97-107.

Carvalho, R.S., 1989. Bacia do Espírito Santo: o "estado da arte" da exploração. *In*: I Sintex – *Seminário de Interpretação Exploratória*, p. 127-134.

Carvalho, M.V.F., De Ros, L.F. & Gomes, N.S., 1995. Carbonate cementation patterns and diagenetic reservoir facies in the Campos Basin Cretaceous turbidites, offshore eastern Brazil. *Marine and Petroleum Geology*, 12: 741–758.

Charef, A., & Sheppard, S.M.F., 1991. The diapir related Bou Grine Pb-Zn deposit (Tunisia): Evidence for role of hot sedimentary basin brines. *In:* Pagel, M. & Leroy, J.L., (Eds.). *Source, Transport and Deposition of Metals*: Proceedings of the 25 Years SGA (Society of Geology Applied to Mineral Deposits) Anniversary Meeting, Nancy, France, 30 August - 3 September 1991: Rotterdam, A. A. Balkema, p. 269-272.

Choquette, P.W. & Pray, L.C., 1970. Geologic nomenclature and classification of porosity in sedimentary carbonates. *AAPG Bulletin*, 54(2): 207-244.

Clayton, R.N. & Mayeda, T.K., 1963. The use of bromine pentafluoride in the extraction of oxygen from oxides and silicates for isotopic analysis. *Geochimica et Cosmochimica Acta*, 27: 43-52.

Cordani, U.G. & Blazekovic, A., 1970. Idades radiométricas das rochas vulcânicas de Abrolhos. *In: Anais XXIV Congresso Brasileiro de Geologia*, v.1, Porto Alegre, p. 265-270.

Daughney, C.J., 2000. Sorption of crude oil from a non-aqueous phase onto silica: the influence of aqueous pH and wetting sequence. *Organic Geochemistry*, 31: 147-158.

Del Rey, A.C. & Zembruscky, S.G., 1991. Estudo hidrogeotérmico das bacias do Espírito Santo e Mucuri. *Boletim de Geociências da PETROBRAS*, 5: 25-38.

Dutton, S., 2008. Calcite cement in Permian deep-water sandstones, Delaware basin, west Texas: origin, distribution and effect on reservoir properties. *AAPG Bulletin*, 92: 765-787.

Ehrenberg, S.N., Skjevrak, I. & Gilje, A.E., 1995. Asphaltene-rich residues in sandstone reservoirs of Haltenbank province, mid-Norwegian continental shelf. *Marine and Petroleum Geology,* 12: 53–69.

Empinotti, T.C., Paraízo, P., Moraes, M.A.S. & Oliveira, T., 2011. An integrated approach for the study of deep-water reservoirs. *AAPG ICE,* Milan, Italy, October 2011. AAPG Search and Discovery Article #90135.

Enos, J.S. & Kyle, J.R., 2002. Diagenesis of the Carrizo sandstone at Butler salt dome, East Texas Basin, U.S.A.: Evidence for fluid-sediment interaction near halokinetic structures. *Journal of Sedimentary Research*, 72: 68-81.

Esch, W.L. & Hanor, J.S., 1995. Fault and fracture control of fluid and diagenesis around the Iberia salt dome, Iberia Parish, Louisiana. *GCAGS Transactions*, 45: 31-45.

Estrella, G., Mello, M.R., Gaglianone, P.C., Azevedo, R.L.M., Tsubone, K., Rossetti, E., Concha, J. & Brüning, I.M.R.A., 1984. The Espírito Santo basin, Brazil: source rock characterization and petroleum habitat. *In:* Demaison, G. & Murris, R.J. (Eds.). *Petroleum Geochemistry and Basin Evaluation*: AAPG Memoir, American Association of Petroleum Geologists, Tulsa, Oklahoma, p. 253-271.

Evans, D.G. & Nunn, J.A., 1989. Free thermohaline convection in sediments surrounding a salt column. *Journal Geophysical Research*, 94: 12413-12422.

Evans, D.G., Nunn, J.A., & Hanor, J.S., 1991. Mechanisms driving ground water flow near salt domes. *Geophysical Research Letters*, 18: 927-930.

Fetter, M., De Ros, L.F. & Bruhn, C.H.L., 2009. Petrographic and seismic evidence for the depositional setting of giant turbidite reservoirs and the paleogeographic evolution of Campos Basin, offshore Brazil. *Marine and Petroleum Geology*, 26: 824-853.

Friedman, G.M., 1959. Identification of carbonate minerals by staining methods. *Journal of Sedimentary Petrology*, 29(1): 87-97.

Friedman, I. & O'Neil, J.R., 1977. Compilation of stable isotopic fractionation factors of geochemical interest. *In:* Fleischer, M., (Ed.). *Data of Geochemistry*, 6th Ed. USGS Professional Paper. United States Geological Survey, 12 pp.

Giles, M.R., Indrelid, S.L., Beynon, G.V., & Amthor, J., 2000. The origin of large-scale quartz cementation: evidence from large data sets and coupled heat- fluid mass transport modelling. *In:* Worden, R.H. & Morad, S. (Eds.). *Quartz Cementation in Sandstones*: IAS Special Publication 29, p. 21-38.

Glasmann, J.R., Lundegard, P.D., Clark, R.A., Penny, B.K., & Collins, I.D., 1989a. Geochemical evidence for the history of diagenesis and fluid migration: Brent sandstones, Heather Field, North Sea. *Clay Minerals*, 24: 255-264.

Glasmann J.R., Clark R.A., Larter S., Briedis N.A. and Lundegard P.D., 1989b. Diagenesis and hydrocarbon accumulation, Brent Sandstone (Jurassic), Bergen High Area, North Sea. *AAPG Bulletin*, 73(11): 1341-1360.

Hancock, N.J., 1987. Possible causes of the Rotliegend sandstone diagenesis in northern West Germany. *Journal of the Geological Society*, London, 135: 35-40.

Hanor, J.S., 1987a. Kilometre-scale thermohaline overturn of pore waters in the Lousiana Gulf Coast. *Nature*, 327: 501.

Hanor, J.S., 1987b. Origin and Migration of Subsurface Sedimentary Brines: SEPM Short Course, v. 21: Tulsa, Society of Economic Paleontologists and Mineralogists, 247 p.

Hart, B.S., Longstaffe, F.J. & Flint, A.G., 1992. Evidence for relative sea level change from isotopic and elemental composition of siderite in the Cardium Formation, Rocky Mountain Foothills. *Bulletim of Canadian Petroleum Geology,* 40: 52-59.

Hayes, M.J. & Boles, J.R., 1992. Volumetric relations between dissolved plagioclase and kaolinite in sandstones: implications for aluminium mass transfer in the San Joaquim Basin. SEPM Special Publication 47, p. 111-124.

Jensenius, J. & Munksgaard, N.C., 1989. Large scale hot water migration systems around salt diapirs in the danish central trough and their impact on diagenesis of chalk reservoirs. *Geochimica et Cosmochimica Acta*, 53(1): 79-87.

Kaldi, J. & Gidman, J., 1982, Early diagenetic dolomite cements: examples from the Permian Lower Magnesian Limestone of England and the Pleistocene carbonates of the Bahamas. *Journal of Sedimentary Petrology*, 52: 1073-1085.

Ketzer, J.M., Morad, S. & Amorosi, A., 2003. Predictive diagenetic clay-mineral distribution in siliciclastic rocks within a sequence stratigraphic framework. *In*: R. Worden and S. Morad (Eds.), *Clay Mineral Cements in Sandstones*. IAS Speial Publication 34, p. 42–59.

Kyle, J.R. & Saunders, J.A., 1997. Metallic deposits of the Gulf Coast basin: diverse mineralization styles in a young sedimentary basin. *In:* Sangster, D.F., (Ed.). *Carbonate-hosted Lead–Zinc Deposits*. Society of Economic Geologists, Littleton, CO, v. 4, p. 218–229.

Light, M.P.R., & Posey, H.H., 1992. Diagenesis and its relation to mineralization and hydrocarbon reservoir development: Gulf Coast and North Sea basins. *In: Diagenesis III*, Developments in Sedimentology 47, Elsevier, p. 511-541.

Machel, H.G., 1987. Some aspects of diagenetic sulphate-hydrocarbon redox reactions. *In:* Marshall, J.D. (Ed.). *Diagenesis of Sedimentary Sequences*: Geological Society Special Publication 36, p. 15-28.

Machel, H.G., 2001. Bacterial and thermochemical sulfate reduction in diagenetic settings - old and new insights. *Sedimentary Geology*, 140: 143-175.

Mansurbeg, H., El-ghali, M.A.K., Morad, S. & Plink-Björklund, P., 2006. The impact of meteoric water on the diagenetic alterations in deep-water, marine siliciclastic turbidites. *Journal of Geochemical Exploration*, 89 (1-3): 254-258.

Mansurbeg, H., De Ros, L.F., Morad, S., Ketzer, J.M., El-ghali, M.A.K., Caja, M.A., & Othman, R., 2012. Meteoric-water diagenesis in late Cretaceous canyon-fill turbidite

reservoirs from the Espírito Santo basin, eastern Brazil. *Marine and Petroleum Geology*, 37: 7-26.

McManus, K.M., & Hanor, J.S., 1988. Calcite and iron sulfide cementation of Miocene sediments flanking the West Hackberry salt dome, southwest Louisiana, U.S.A. *Chemical Geology*, 74(1-2), Fluid-Rock Interactions in the Salt Dome Environment, p. 99-112.

McManus, K.M., & Hanor, J.S., 1993. Diagenetic evidence for massive evaporite dissolution, fluid flow, and mass transfer in the Louisiana Gulf Coast. *Geology*, 21: 727–730.

Morad, S., Ketzer, J.M., & De Ros, L.F., 2000. Spatial and temporal distribution of diagenetic alterations in siliciclastic rocks: implications for mass transfer in sedimentary basins. *Sedimentology*, 47: 95-120.

Morad, S., Al-Ramadan, K., Ketzer, J.M., De Ros, L.F., 2010. The impact of diagenesis on the heterogeneity of sandstone reservoirs: A review of the role of depositional facies and sequence stratigraphy. *AAPG Bulletin*, 94: 1267-1309.

Morad, S., Ketzer, J.M. & De Ros, L.F., 2012. Linking diagenesis to sequence stratigraphy: an integrated tool for understanding and predicting reservoir quality distribution. *In:* Morad, S., Ketzer, J.M. & De Ros, L.F. (Eds.). *Linking Diagenesis to Sequence Stratigraphy*, IAS Special Publication 45, Chichester, UK, International Association of Sedimentologists, Wiley-Blackwell, p. 1-36.

O'Brien, J.J., & Lerche, I., 1987. Heat flow and thermal maturation near salt diapirs. *In:* Lerche, I., & O'Brien, J.J. (Eds.). *Dynamical Geology of Salt and Related Structures*: Orlando, Florida, Academic Press, p. 711–750.

Posey, H.H., & Kyle, J.R., 1988. Fluid-rock interactions in the salt dome environment: an introduction and review. *Chemical Geology*, 74(1-2) Fluid-Rock Interactions in the Salt Dome Environment, p. 1-24.

Posey, H.H., Kyle, J.R., & Agee Jr., W.N., 1994. Relations between diapiric salt structures and metal concentrations, Gulf Coast sedimentary basin, southern North America. *In:* Fontbote, L., & Boni, M. (Eds.). *Sediment-hosted Zn–Pb Ores*: Berlin, Springer-Verlag, p. 139–164.

Prochnow, E.A., Remus, M.V.D., Ketzer, J.M., Gouvea Jr., J.C.R., Schiffer, R. & De Ros, L.F., 2006. Organic-inorganic interactions in oilfield sandstones: examples from turbidite reservoirs in the Campos basin, offshore eastern Brazil. *Journal of Petroleum Geology*, 29: 361-380.

Ranganathan, V., & Hanor, J.S., 1988. Density-driven groundwater flow near salt domes. *Chemical Geology*, 74(1-2): Fluid-Rock Interactions in the Salt Dome Environment, p. 173-188.

Rashid, M.A., 1978. The influence of a salt dome on the diagenesis of organic matter in the Jeanne d'Arc sub-basin of the northeast Grand Banks of Newfoundland. *Organic Geochemistry*, 1(2): 67-77.

Rosenbaum, J.M. & Sheppard, S.M.F., 1986. An isotopic study of siderites, dolomites and ankerites at high temperatures. *Geochimica et Cosmochimica Acta*, 50: 1147-1150.

Rossi, C., & Cañaveras, J. C., 1999. Pseudospherulitic fibrous calcite in paleo-groundwater, unconformity-related diagenetic carbonates (Paleocene of the Ager Basin and the Miocene of the Madrid Basin, Spain). *Journal of Sedimentary Research*, 69: 224–238.

Schmidt, V., & McDonald, D.A., 1979. The role of secondary porosity in the course of sandstone diagenesis. *In:* Scholle, P.A. & Schluger, P.R. (Eds.). *Aspects of Diagenesis*, SEPM Special Publication 29, Society of Economic Paleontologists and Mineralogists, Tulsa, Oklahoma, p. 175-207.

Sharp, J.M., Fenstemaker T.R., Simmons, C.T., McKenna, T.E., & Dickinson, J.K., 2001. Potential of salinity-driven free convection in a shale-rich sedimentary basin: example from the Gulf of Mexico basin in South Texas. *AAPG Bulletin*, 85: 2089–2110.

Surdam, R.C., Dunn, T.L., Heasler, H.P., & MacGowan, D.B., 1989. Porosity evolution in sandstone/shale systems. *In:* Hutcheon, I.E. (Ed.). *Short Course on Burial Diagenesis*: Mineralogical Association of Canada Short Course Handbook 15, p. 61–133.

Ulrich, M.R., Kyle, J.R., & Price, P.E., 1984. Metallic sulfide deposits in the Winnfield salt dome, Louisiana: evidence for episodic introduction of metalliferous brines during cap rock formation. *Transactions Gulf Coast Association of Geological Societies*, 34: 435–442.

Vennemann, T.W. & O'Neil, J.R., 1993. A simple and inexpensive method of hydrogen isotope and water analyses of minerals and rocks based on zinc reagent. *Chemical Geology*, 103: 227-234.

Vieira, P.E., Biassusi, A.S., Brandão, J.R., 1999. Arcabouço preditivo de fácies arenosas no Terciário *offshore* da Bacia do Espírito Santo. *In:* Simpósio sobre Turbiditos 2, Rio de Janeiro, 1999. Boletim de Resumos Expandidos. Rio de Janeiro: PETROBRAS / SEREC / CEN-SUD, p. 66-70.

Wilhelms, A., Larter, S.R., Head, I., Farrimond, P., Di Primio, R. & Zwach, C., 2001. Biodegradation of oil in uplifted basins prevented by deep-burial sterilization. *Nature*, 411: 1034-1037.

Vennemann, T.W. & O'Neil, J.R., 1993. A simple and inexpensive method of hydrogen isotope and water analyses of minerals and rocks based on zinc reagent. *Chemical Geology*, 103: 227-234.

Wilson, M.D. & Stanton, P.T., 1994. Diagenetic mechanisms of porosity and permeability reduction and enhancement. *In: Reservoir Quality Assesment and Prediction in Clastic Rocks*, SEPM Short Course Notes 30, p. 59-117.

9. ARTIGO SUBMETIDO – METEORIC AND SALT-DOME RELATED DIAGENESIS IN TERTIARY TURBIDITE RESERVOIRS FROM THE ESPIRITO SANTO BASIN, BRAZIL

JSR 2017-185 Receipt of New Paper by the Journal of Sedimentary Research

Dear Authors,

Manuscript 2017-185 entitled "METEORIC AND SALT DOME-RELATED DIAGENESIS IN TERTIARY TURBIDITE RESERVOIRS FROM THE ESPÍRITO SANTO BASIN, BRAZIL", of which you are listed as a coauthor, has been approved for review by the Journal of Sedimentary Research.

You may check on the status of this manuscript by selecting the "Check Manuscript Status" link at the following URL:

http://sepm-jsr.allentrack.net/cgi-bin/main.plex?el=A7BE1Cbq1A2HIo6F1A9ftd61Z2WY6QckapjbSWnxdzxwZ

(Press/Click on the link above to be automatically sent to the web page. Please note that these links may be too long to fit on one line and may need to be pasted into your browser separately.)

Very sincerely,

Gary Hampson, Leslie Melim
Co-Editors
JSR

This email was generated by AllenTrack, the electronic submission & review site for JSR. If there are any errors or missing attachments, please email the editorial office, jsedres@gmail.com. Thank you!

METEORIC AND SALT DOME-RELATED DIAGENESIS IN TERTIARY TURBIDITE RESERVOIRS FROM THE ESPÍRITO SANTO BASIN, BRAZIL

DANIEL M. OLIVEIRA[1] AND LUIZ FERNANDO DE ROS[2]

1 Petrobras Research Center - Rio de Janeiro, Brazil

2 Institute of Geosciences, Federal University of Rio Grande do Sul - Porto Alegre, Brazil

E-mail address: danielmoliv@petrobras.com.br (corresponding author)

Key words: meteoric incursion; salt dome-related diagenesis; thermobaric regime; kinetic constraints; turbidite reservoirs.

ABSTRACT

The diagenetic evolution of two tertiary turbidite reservoirs from the offshore portion of the Espírito Santo Basin, eastern Brazil, was influenced by the flow of meteoric and salt dome-related fluids, which had different impacts on their quality. Marine eogenetic processes included the precipitation of framboidal pyrite, microcrystalline dolomite and siderite. Meteoric water influx during eodiagenesis occurred in response to relative sea-level falls that promoted extensive kaolinization ($\delta^{18}O$=+15.3‰ to +18.2‰; δD= -51‰ to -66‰) and dissolution of framework silicate grains. During progressive burial (present depths = 2600 m – 3000 m), marine fluids modified by reactions with organic matter and carbonates derived from the surrounding mudrocks gradually displaced the brackish fluids generated by the meteoric influx and promoted concretionary cementation by poikilotopic calcite ($\delta^{18}O_{VPDB}$= -10.23‰ to -4.30‰; $\delta^{13}C_{VPDB}$=-3.59‰ to 1.76‰). Mesogenetic fluids were progressively modified by the proximity of salt domes, which led to ubiquitous feldspar albitization and localized quartz, calcite ($\delta^{18}O_{VPDB}$=-10.66‰ to -9.86‰; $\delta^{13}C_{VPDB}$=-5.90‰ to -3.70‰) and saddle dolomite precipitation ($\delta^{18}O_{VPDB}$= -6.5 ‰ to -11.7 ‰; $\delta^{13}C_{VPDB}$=-1.43 ‰ to -5.48 ‰). Fluid inclusions in quartz overgrowths indicate that the precipitating fluids had salinities predominantly in the range 8-13 wt% NaCl equivalent and temperatures largely in the 100 – 155°C range. These values are higher than those expected considering the normal geothermal gradient for the studied area. The distribution of feldspar albitization suggests that the fracture systems along the margins of the salt domes acted as preferential pathways for such hot, saline diagenetic fluids. $\delta^{13}C$ and $\delta^{18}O$ values of calcite and dolomite cements follow a decreasing co-variance trend from close to marine (~0‰) towards negative values

($\delta^{13}C$ and $\delta^{18}O$ down to -5.9‰ and -10.9‰ for calcite; -5.4‰ and -11.7‰ for dolomite), suggesting increasing contribution from thermal decarboxylation with increasing temperature and depth. Mechanical compaction was more important than cementation in reducing depositional porosity, and the dissolution of framework silicate grains is the most important processes for enhancing reservoir quality. The influence of the salt domes on the diagenetic processes of the reservoirs was relatively mild, despite their proximity, as pore-filling neoformed illite is absent, and quartz cement occurrence is limited in the sandstones, what that may be related to the late burial of the reservoirs. This study shows that the prediction of salt dome-related diagenesis and reservoir quality is a function of multiple variables, including the dimensions of the salt dome, the regional thermal regime of the basin, the thermal and fluid conductivity, and the mineral composition and geomechanical properties of the reservoirs and associated lithologies. We expect to contribute to the understanding and prediction of diagenesis and reservoir properties of turbidite sandstones influenced by meteoric and salt dome-related fluids in offshore Espírito Santo Basin and in other similar areas.

INTRODUCTION

The understanding of the distribution of diagenetic processes and products is of major importance for the characterization of the quality and heterogeneity of clastic reservoirs (Morad et al., 2000; Morad et al., 2010). That is, however, a complex task, since diagenesis is governed by numerous inter-related parameters, such as detrital composition, depositional facies, climatic conditions, tectonic settings and burial history, which in turn govern the fluid chemical composition and flow patterns (Wilson and Stanton, 1994; Morad et al., 2000).

In general, the influence of diagenesis in turbidite reservoirs is relatively poorly understood, and believed to be essentially mediated by marine pore waters (Bjorlykke and Aagard, 1992;

Dutton, 2008). In the past decades, offshore hydrocarbon exploration has been increasingly concentrated in marine, turbiditic sandstone reservoirs deposited in basins situated along passive continental margins. In Brazil, despite the new discoveries of pre-salt deposits, deep-water turbidites reservoirs are still major exploration targets, since they still correspond to a substantial portion of the oil production. An extensive database and a wide comprehension of Brazilian turbidite reservoirs have been generated through sedimentological, stratigraphic and architectural studies (Bruhn, 2001; Fetter *et al.,* 2009; Empinotti *et al.,* 2011). However, the advance of exploration activities enhances the demand for more studies regarding the diagenetic controls on turbidite reservoir quality, since the reservoirs yet to be discovered are influenced by more complex and intense diagenetic modifications.

In the last years, the role and influence of meteoric water incursion on diagenetic alterations, and hence on reservoir quality of turbidite sandstones, have been pointed out by some authors (Mansurberg et al., 2006; Prochnow et al., 2006; Mansurberg et al., 2012). Also, the influence of salt-domes on the distribution of diagenetic products and processes in sandstones has already been recognized (McManus and Hanor, 1988; 1993; Posey and Kyle, 1988; Posey *et al.*, 1994; Esch and Hanor, 1995; Enos and Kyle, 2002; Bruno and Hanor, 2003; Archer et al., 2004). This study aims to present and discuss the controlling parameters involved in meteoric- and salt dome-related diagenetic processes affecting two Tertiary turbidite reservoirs from offshore Espírito Santo Basin, eastern Brazil. The understanding of the controls on the quality of these reservoirs shall contribute to the assessment of risks involved in the exploration for equivalent turbidite reservoirs in the Espírito Santo Basin and other locations with similar geological situation.

GEOLOGICAL SETTING

The Espírito Santo Basin, eastern Brazil margin, was generated in the Eocretaceous by the Neocomian breakup of Gondwanaland, and developed during the subsequent opening of the South Atlantic Ocean, which resulted in the separation and drifting of the African and South American plates. The Espírito Santo Basin covers an area of about 25,000 Km^2 and is bordered by the Mucuri Palaeocanyon to the north, the Vitória High to the south, the Abrolhos Volcanic Complex to the east, and by the Precambrian crystalline basement to the west. The latter is composed of migmatites, granulites, gneisses and granites, which occur as homoclinal, faulted blocks tilted towards the east (Del Rey and Zembruscky, 1991) (**Fig. 1**).

The main source rocks in the basin are Neocomian rift phase lacustrine shales of the basal Cricaré Formation (Estrella et al., 1984; Carvalho, 1989), which are covered by Aptian alluvial sandstones and conglomerates of the Mucuri Member from the Mariricu Formation. After the deposition of Mucuri Member, a marine incursion under restricted circulation conditions and arid climate precipitated the thick sequence of Aptian evaporites of the Itaúnas Member from the Mariricu Formation, characterized by the intercalation of anhydrite, halite and potassium salt strata. Shallow marine carbonates (Regência Member) and fan-deltaic clastics (São Mateus Member) of the Barra Nova Formation were deposited during the Albian-Cenomanian.

During the Neocretaceous and Paleogene, thermal subsidence and tilting of blocks towards the east, and related salt tectonics controlled the deposition of the thick sequence of marine muds and turbiditic sands of the Urucutuca Formation. In the northern part of the basin, intraplate basic alkaline volcanism began by the end of Neocretaceous, peaking during the Eocene (37 m.y.; Cordani and Blazekovic, 1970), building the large Abrolhos volcanic platform.

The studied area comprises two petroleum fields, Cangoá and Peroá, respectively of Eocene and Oligocene age, which are located in the "salt dome province" (about 40 km far

from the coast), southern part of the basin (**Fig. 2**). The deposition of Urucutuca turbidites in this area occurred dominantly as a complex of channelized sand bodies, deposited at the base of the slope, along depressions generated by the Aptian salt diapirism.

Despite their age difference, the Cangoá and Peroá turbiditic sandstones are both limited by regional unconformities (**Fig.3**) and deposited under control by active tectonism, which promoted the transport of first-cycle alluvial and fluvial sediments to deep basinal settings, as indicated by their compositional and textural immaturity. An analogous situation is observed in most of the giant turbidite reservoirs from Campos Basin (Fetter *et al.*, 2009).

STRUCTURE OF THE FIELDS

The studied fields are located within the "salt dome province", characterized by structures produced by the halokinesis of the Aptian evaporites and their active piercement of younger successions. Such halokinesis, initiated during the Albian as consequence of structural tilting and progradation of a mixed carbonate-siliciclastic succession, exerted important control on the distribution, accumulation and diagenetic evolution of turbiditic deposits in the Cangoá and Peroá areas.

The Cangoá Field is located at the northwestern flank of a salt dome. A time slice seismic image reveals a system of concentric fractures affecting the surrounding sandstones and mudrocks (**Fig. 4**). The salt dome acted as a barrier for the turbidite flows, as shown by the pinching of the sand bodies towards the dome. The halokinesis deformed Eocene strata and influenced the initial diagenetic evolution of the reservoir.

The structural context of Peroá Field is unique among all the fields from Espírito Santo Basin. Although halokinesis played an important role on reservoir distribution, it was apparently less important in its compartmentalization. Differently to what is observed in Cangoá, the reservoirs of Peroá are not in direct contact with a salt dome. The structure of Peroá Field is related to mechanisms of differential compaction of the sandstones and the surrounding

mudrocks above a compressional structural high (Vieira *et al.*, 1999). Such large structure, previously interpreted as a salt dome, was revealed by drilling to be a thick thrusted wedge of cretaceous mudrocks (**Fig.3**). Such discovery motivated a debate on whether the salt diapirism was the cause or a product of the compressional regional tectonics observed in the studied area.

SAMPLES AND ANALYTICAL METHODS

Altogether, ninety samples from six wells cored through the Urucutuca Formation (four in Cangoá and four in Peroá Field) were selected for this study. Modal compositions and paragenetic interpretations of the sandstones were obtained through systematic quantitative petrography, by counting 300 points in each thin section prepared from samples impregnated with blue epoxy resin. Staining with hydrochloridric solution of alizarin Red-S and potassium ferrocyanide was performed in order to differentiate the carbonate minerals (cf. Friedman, 1959). Scanning electron microscopy (SEM) secondary and backscattered electrons (BSE) analyses were performed in a JEOL JSM-6690LV microscope for a better definition of the paragenetic relationships among primary and diagenetic constituents and porosity on selected samples and thin sections, with support from an Oxford-Inca energy dispersive spectrometer (EDS) for the identification of the elemental composition of the constituents.

X-ray diffraction (XRD) analyses of 2µm selected fractions were performed for the identification of the clay minerals present in 69 samples (6 sandstones and 63 mudrocks), using a Rigaku D/MAX – 2200/PC diffractometer under the following operating conditions: 40 mA and 40 kV, and 2mm, 0.3mm and 0.6mm slit sizes. The samples were air-dried, ethylene glycol-saturated and heated at 490°C for 4 hours.

Stable carbon and oxygen isotope analyses were conducted in carbonate cements of 17 sandstone samples at the Laboratory for Isotopic Studies from the University of Windsor. Samples containing both calcite and dolomite were analyzed through the chemical fractionation method of Al-Aasm *et al.* (1990). The samples were reacted in vacuum with 100% H_3PO_4 for four hours at 25° and 50°C for calcite and dolomite, respectively. The evolved CO_2 gas was analyzed for isotopic ratios on a Delta Plus mass spectrometer. The phosphoric acid fractionation factors used were 1.01025 for calcite (Friedman and O'Neil, 1977) and 1.01060 for dolomite (Rosenbaum and Sheppard, 1986). Delta (δ) values for oxygen and carbon are reported in per mil (‰) relative to the Vienna Pee Dee Belemnite (VPDB) standard. Precision is better than ±0.05‰ for both $\delta^{18}O$ and $\delta^{13}C$.

Stable oxygen and hydrogen isotopes of kaolinite were obtained from 7 sandstone samples at the Laboratory for Stable Isotope Science of the University of Western Ontario. The results are reported in per mil (‰) relative to the Vienna Standard Mean Ocean Water (V-SMOW) standard. The samples were powdered, separated in different fractions and analyzed through X-ray diffraction (XRD) in order to identify the fraction containing the greater amount of kaolinite. Dried samples were heated and pumped in Ni-reaction vessels under vacuum at 300°C for 2 h prior to reaction with ClF_5. The samples were reacted at 580°C overnight. Oxygen was extracted from the silicates using the method of Clayton and Mayeda (1963), modified to use ClF_3 and converted quantitatively to CO_2 over red-hot graphite. Samples were analyzed on either an Optima or a Prism dual inlet mass spectrometer using NBS-28 to calibrate in-house quartz and clay standards. Sample reproducibility is generally better than ±0.3‰. Hydrogen was extracted from kaolinite following the procedure of Bigeleisen et al. (1952), modified by Vennemann and O'Neil (1993). Samples were first dried overnight at 105°C under vacuum, and then heated to ~1200°C using an oxygen-propane torch. The hydroxyl groups were converted to H_2O by reaction with copper oxide at 400-600°C, and the H_2O was then reduced to H_2 gas over Cr

at 900°C. Stable hydrogen-isotope compositions were measured using the VG Prism-II stable isotope ration mass-spectrometer calibrated to VSMOW and SLAP using four in-house water standards. Sample reproducibility was generally better than $\pm$5‰.

Five core samples were selected for fluid inclusion analysis aiming to determine trapping temperatures and salinities of aqueous inclusions in quartz cements. The samples were examined both with transmitted light and under UV illumination at FIT Inc. laboratory. Fluid inclusion assemblages were selected according to their relationship to the host mineral, consistency of visual parameters (e.g. apparent liquid/vapor ratio) and applicability for determining the information. Aqueous and oil inclusion homogenization temperatures and aqueous inclusion salinities were determined with a modified U.S.G.S. heating-freezing stage using standard techniques.

RESULTS

Composition, Provenance and Modifications of Framework Grains

The sandstones are in general moderately to poorly-sorted and medium- to coarse-grained. Very poorly sorted, very coarse-grained and conglomeratic sandstones occur rarely, usually at the bottom of turbidite cycles. The sandstones original essential composition corresponds to arkoses *sensu* Folk (1968) (**Fig. 5A**; average QFL). However, due to the ubiquitous albitization and kaolinization, and to the extensive dissolution of feldspar grains, all the samples show a shift towards the subarkose field in Folk classification diagram (**Fig. 5A**). This essential primary composition corresponds to the uplifted basement and transitional continental provenance detrital modes of Dickinson (1985) diagram (**Fig. 5B**), indicating that the sediments were rapidly eroded from uplifted plutonic terrains of the Serra do Mar (Coastal Range), and transported into the basin by alluvial systems directly to turbidite currents.

Quartz is the dominant detrital constituent and occurs dominantly as monocrystalline grains (**Table 1**). Among the feldspars, plagioclase dominates over microcline, orthoclase and perthite (**Table 1**). Untwinned, medium-grade metamorphic plagioclase grains are commonly fresh, while twinned plagioclase grains are extensively albitized and commonly replaced by calcite (**Table 1**). Lithic fragments are almost exclusively plutonic, with trace amounts of low-grade metamorphic fragments (**Table 1**). Some samples were originally rich in micas (muscovite and biotite), although their present amount is reduced mostly due to extensive muscovite kaolinization (**Table 1**).

Other primary constituents include heavy minerals (mostly garnet, zircon and opaque minerals), mollusk, equinoid, benthic foraminifera and macroforaminifera carbonate bioclasts, mud intraclasts and carbonaceous fragments. Garnet grains commonly show partial dissolution.

Mud intraclasts occur usually in trace amounts, but may be concentrated in some intervals, being commonly compacted to pseudomatrix. The common presence of nannofossils in mud intraclasts suggests that these were eroded from slope deposits. Both intraclasts and pseudomatrix are locally replaced by cryptocrystalline to microcrystalline silica. Carbonaceous fragments occur mainly associated to mica flakes, due to their hydraulic equivalence.

Diagenesis

The main diagenetic minerals identified are here described in their order of abundance, as shown in **Table 1**.

Albite

Albite is the most abundant authigenic constituent in the studied sandstones (**Table 1**), occurring essentially replacing the detrital feldspars. Albite habits and microtextural

characteristics are controlled by the types of replaced feldspars (Saigal et al., 1988; Morad et al., 1990). Albitization was, in many cases, initiated along twinning, cleavage or micro-fracture planes, continuing commonly to pervasive replacement of the feldspar grains. Albitization of orthoclase and twinned plagioclase was commonly pervasive and in some cases associated with their partial dissolution (**Fig. 6A; 6B and 6C**). Untwinned plagioclase and microcline are commonly not replaced (**Fig. 6A and 6D**) or only slightly albitized, dominantly along grains margins and fractures. Albite that has replaced twinned plagioclase occurs either as cryptocrystalline aggregates or as parallel prismatic microcrystals (ca. <50μm), which optical orientation commonly mimics the host polysynthetic twinning. Albitization of orthoclase grains is characterized by patchy microdomains of cryptocrystalline aggregates (cf. Morad, 1986; Morad *et al.*, 1990).

Albite overgrowths around plagioclase grains are either untwinned or display orientation following their host polysynthetic twining, whereas those around albitized K-feldspar grains are generally untwinned (**Fig. 6A and 6D**). Albite overgrowths are engulfed by, and hence pre-date, late calcite and dolomite cement.

Kaolinite

Kaolinite is the dominant clay mineral in the sandstones, occurring as grain-replacive and, less commonly, as intergranular pore-filling (Table 1). Kaolinite replaces feldspar, micas, mud intraclasts and pseudomatrix. Kaolinite authigenesis is mostly related to the dissolution of feldspar grains (**Fig. 6E**). Mica grains that are replaced by kaolinite, were expanded into adjacent pores and display the typical fan-like shape (**Fig. 6D and 6F**). Kaolinite that has replaced feldspars occurs as aggregates of vermicular and booklet-like crystals that are rich in intercrystalline porosity (**Fig. 6E, 7A and 7B**), whereas patches that have resulted from the kaolinization of mica and, particularly, mud intraclasts contain smaller amounts of micro-porosity. Kaolinite that replaces mud intraclasts and compactional pseudomatrix shows

variable but overall smaller size (ca. 3 µm) than kaolinite that replaced micas and feldspars. Kaolinite is more abundant in the facies where grain fracturing was pronounced.

The oxygen and hydrogen isotopic values of kaolinite vary between $\delta^{18}O_{VSMOW}$ +15.3 ‰ and +18.2 ‰ and δD_{VSMOW} – 51 ‰ and – 66 ‰ respectively.

Calcite

Calcite occurs both as early, pre- to sin-compactional, and as late, post-compactional, varieties. Early calcite shows concretional distribution and macrocrystalline to poikilotopic habits (**Fig. 7C**), filling intergranular pores (**Table 1**), expanding biotite flakes and partially replacing framework grains and diagenetic kaolinite, pyrite and dolomite (**Fig. 6F; 7B; 7C and 7D**). The large intergranular volumes and very loose packing of the sandstones cemented by early calcite indicate that such cementation occurred at shallow burial depths, prior to significant compaction. $\delta^{18}O_{VPDB}$ values for early calcite vary between -10.23‰ and -4.30‰, and $\delta^{13}C_{VPDB}$ values between -3.59‰ and 1.76‰ (**Table 2**).

Post-compactional late calcite has macrocrystalline to poikilotopic habits, replaces framework grains and engulfs, and hence post-dates, albite and quartz overgrowths, and late dolomite crystals (**Fig. 6A and 7E**). Such calcite is locally ferroan and commonly the latest diagenetic phase in the studied sandstones. $\delta^{18}O_{VPDB}$ values of late calcite vary between -10.66‰ and -9.86‰ and $\delta^{13}C_{VPDB}$ values between -5.90‰ and -3.70‰ (**Table 2**).

Dolomite

Dolomite, likewise calcite, occurs as both early and late diagenetic phases. Early dolomite occurs with microcrystalline habit, expanding and replacing biotite flakes and locally filling intergranular pores. Early dolomite is typically associated with microcrystalline and framboidal pyrite (**Fig. 7C and 7F**).

Late dolomite occurs with ferroan (**Fig. 7E**) and non-ferroan composition, with coarse macrocrystalline habit and locally as crystals with wavy extinction and curved defective faces ("saddle dolomite"; **Fig. 8A**). Late dolomite fills pores reduced by mechanical compaction, but also replaces framework grains and engulfs albite and quartz overgrowths, and kaolinite aggregates. The $\delta^{13}C_{VPDB}$ values for late dolomite vary from -1.43 ‰ to -5.48 ‰. The $\delta^{18}O_{VPDB}$ values vary from -6.5 ‰ to -11.7 ‰ (**Table 2**).

Quartz

Diagenetic quartz is volumetrically subordinate in the sandstones, occurring mainly as syntaxial overgrowths (**Table 1**) (**Fig. 8B**) and as ingrowths healing microfractures in detrital quartz grains (**Fig. 6B and 8C**). Quartz overgrowths, which engulf and hence post-date kaolinite (**Fig. 7A and 8D**), are more abundant in sandstones devoid of early calcite cement. Albite overgrowths either envelop, or are enveloped by, quartz overgrowths, thus indicating that they are co-genetic at some scale. Quartz overgrowths are partly replaced by, and thus pre-date, late dolomite and calcite (**Fig. 6A and 7E**).

A summary of the microthermometry analyses of quartz fluid inclusions in Cangoá and Peroá sandstones is presented in **Table 3**. The homogenization temperatures (T_h, which record the minimum temperature under which the inclusion may have formed) of aqueous and oil inclusions range broadly from 115 to 145°C. Data suggest that oil inclusions formed between 115-135°C, whereas aqueous inclusions have temperatures largely in the range 100-119°C for the sample from PER-A, 110-146°C for samples from CAN-C, and 125-155°C for samples from CAN-A well. Salinities are predominantly in the range of 8 to 13 wt% NaCl equivalent.

Other diagenetic minerals

Mud intraclasts and pseudomatrix derived from their compaction are locally replaced by microporous cryptocrystalline silica (**Fig. 8E**), as documented in other turbidite sandstones

from eastern Brazilian margin basins and abroad (Sears, 1984; Moraes, 1989; van Benekkon et al., 1989; Carvalho et al., 1995).

Other diagenetic minerals include siderite, pyrite, K-feldspar, apatite and tourmaline. Microcrystalline siderite occurs in a few samples and usually replaces and expands biotite flakes. Pyrite displays framboidal and microcrystalline habit, mainly expanding and replacing biotite, and locally filling intraparticle pores in carbonate bioclasts (**Fig. 8F; 9A and 9B**). Titanium oxides replace heavy mineral grains and surround moldic pores originated by their dissolution. K-feldspar overgrowths are scarce, covering discontinuously microcline grains in a few samples.

Exotic and rare occurrences include poikilotopic apatite filling intergranular pores, and tourmaline overgrowths.

Compaction and Porosity

The formation of pseudomatrix from plastic deformation of mud intraclasts and the bending of mica plates are the most obvious features indicative of mechanical compaction in the studied sandstones (**Fig. 8F and 9C**). However, most of the fracturing observed in quartz and feldspar grains (**Fig. 9D and 9E**) was probably not related to mechanical compaction, since it occurs heterogeneously, discontinuously and limited to some grains, in certain intervals of the wells, suggesting that this fracturing was promoted by shallow tectonism pre-dating the lithification of the turbiditic deposits (Makowitz and Milliken, 2003). Feldspar grain dissolution was commonly pronounced in some samples with such early fracturing (**Fig. 6E and 9E**).

Chemical compaction was in general limited, except along the contacts with mica flakes and carbonaceous fragments, where pressure dissolution was apparently catalyzed, with the development of stylolitic surfaces along some intervals enriched in these grains (**Fig. 8C; 8F and 9A**).

The main pore types in the studied sandstones include intergranular, intragranular and moldic types. In general, intergranular porosity is more abundant than intragranular and moldic pores together (**Table 1**). However, in some samples, secondary porosity due to grain dissolution may constitute up to 25% of total porosity.

Significant microporosity was generated due to feldspar kaolinization.

Clay mineral XRD analytical data

Total amount of clay minerals in analyzed sandstone samples is less than 5wt% and corresponds to mud intraclasts and pseudomatrix, and mostly to authigenic kaolinite (35 - 65%; average: 50% of total clay fraction). Mud intraclasts and pseudomatrix are composed of illite-smectite mixed-layer (**Fig. 9F**) (average: 30%; min: 20%; max: 50% of total clay fraction), and chlorite (average: 20%; min: 12%; max: 35% of total clay fraction).

In the mudrock samples, kaolinite is the most abundant clay mineral (23 – 60%; average 39% of total clay fraction) closely followed by illite-smectite mixed-layer (19 – 62%; average 37% of total clay fraction). Chlorite corresponds to 24% average of the total clay fraction and presents a higher variable distribution (6-40%).

DISCUSSION

The petrographic evidence suggests that the evolution of the studied sandstones took place during eodiagenesis and mesodiagenesis (*sensu* Choquette and Pray, 1970; Schmidt and McDonald, 1979). Stable isotope analyses of carbonate cements and of authigenic kaolinites, together with analyses of fluid inclusions in quartz overgrowths and with the paragenetic relations among diagenetic processes and products, as well as with the detrital constituents and with the porosity, helped constraining the paragenetic sequence (**Fig. 10**) and the temperature and composition of the related diagenetic fluids.

The following discussion will show that during eodiagenesis, the turbiditic succession was influenced both by marine and meteoric (brackish) fluids, while during mesodiagenesis compactional fluids derived from the surrounding mudrocks were progressively displaced by formation waters geochemically evolved owing to the interaction with the salt domes. The terminology adopted for the diagenetic stages also incorporates the definition of Galloway (1984) for the hidrogeologic regimes.

Marine eodiagenesis

The earliest recognized diagenetic processes include the precipitation of small amounts of pyrite, dolomite and siderite replacing biotite flakes and mud intraclasts, and filling intraparticle pores in foraminifera. Despite the lack of isotope analysis, the occurrence, habit and paragenetic relations of such minerals (i.e., expanding biotite and filling intraparticle pores previous to pre-compactional early calcite cementation) suggest that their precipitation commenced near the seafloor and took place through iron and sulphate reduction processes due to the action of bacterial metabolism on connate marine fluids (Berner, 1981, 1984; Morad, 1998). The localized precipitation of continuous but thin K-feldspar overgrowths, recorded in few samples, was probably related to marine eogenetic conditions as well.

Early grain fracturing

The heterogeneous distribution of fractured grains suggests that their brittle deformation occurred due to stress at fairly shallow depths, before significant lithification (Makowitz and Milliken, 2003), and may has been related to the movement of the adjacent salt domes. In Cangoá field, turbiditic deposits pinch towards the salt dome, which suggests that halokinesis seems to have controlled both the deposition of the turbidite sands and their initial deformation.

Such salt dome-related fracturing can potentially create clean and "fresh" mineral surfaces, which may either lead to preferential dissolution or precipitation, depending on the saturation of the involved mineral phases (Reed and Laubach, 1996; Milliken and Laubach, 2000). In many samples, the fractured grains were partially to extensively 'healed' by quartz or albite ingrowths developed later during mesodiagenesis. In other samples, fracturing of feldspar grains enhanced dissolution and kaolinization during meteoric eodiagenesis.

Meteoric eodiagenesis

The dissolution and kaolinization of feldspars, micas and mud intraclasts, and the expansion of mica flakes by kaolinite recorded in the studied sandstones were identified in other turbiditic successions in Brazil and abroad, and attributed to meteoric water circulation (Moraes, 1989; Carvalho *et al.*, 1995; Prochnow *et al.*, 2006; Mansurbeg *et al.* 2008; 2012). The presence of high concentrations of dissolved cations, as K^+, Na^+, Ca^{+2} and Mg^{+2} in marine pore waters excludes the possibility of feldspar kaolinization and dissolution by such waters (Berner, 1978). The expansion of kaolinized micas, which indicates the shallow diagenetic origin of kaolinite (Ketzer et al., 2003), excludes the involvement of organic acids (Surdam et al., 1984). Furthermore, stable oxygen and hydrogen isotopes of the kaolin ($\delta^{18}O_{VSMOW}$ +15.3 ‰ to +18.2 ‰ and δD_{VSMOW} – 51 ‰ to – 66 ‰) fall close to the kaolinite meteoric water line (**Fig. 11**), hence supporting a meteoric origin (Savin and Epstein, 1970; Sheppard and Gilg, 1996; Morad et al., 2003). The eogenetic origin of kaolinite in the Urucutuca sandstones is further indicated by the engulfment of intergranular pore-filling kaolinite by pre-compactional calcite cement. Brackish fluids derived from mixing of meteoric water would have influenced part of the carbonate cementation occurring during early subsequent compactional diagenesis, as indicated by stable isotope data and discussed in the next section.

The circulation of considerable volumes of meteoric water into marine turbiditic deposits and the mechanism of meteoric water flow into deep marine successions are yet to be fully understood (Morad et al., 2000). In the present case study, such meteoric influx would have been favored by the creation of a hydraulic head along the basin margin during shallow burial (Deming and Nunn, 1991), in response to the significant uplift of the coastal mountain range (Serra do Mar) during the Eocene (Gallagher et al., 1995, 1999; Tello Saenz et al., 2003, 2005), and may have been mixed with, rather than totally displaced, the marine connate fluids in the turbiditic sands (Ketzer et al., 2003). The top and the bottom boundaries of the turbidite reservoir intervals are characterized, both in Cangoá and Peroá, by significant unconformities developed in response to base-level falls, which could have led to the expansion of the recharge area and thus to the increment of meteoric water influx. The probable conduits for the meteoric waters to the Urucutuca sandstones would correspond to the contacts of the channelized turbidite sand bodies with large and deep regional fault systems.

Compactional mesodiagenesis

During progressive burial, marine fluids modified by reactions involving organic matter and carbonates that took place in the surrounding mudrocks gradually displaced the brackish fluids generated by meteoric water influx in the sandstones. Such interpretation is supported by the distribution, chemical composition and isotopic signatures of the carbonate cements. Particularly, macrocrystalline and poikilotopic calcite was precipitated after the shallow tectonic fracturing and grain kaolinization, but before a significant compaction in the studied sandstones. Fairly negative values for $\delta^{18}O_{VPDB}$ obtained from some of these pre-compactional calcites would have been still influenced by brackish fluids, while the $\delta^{13}C_{VPDB}$ values would be recording the dominance of marine carbonate source from the mudrocks (**Fig.12**).

The replacement of mud intraclasts and pseudomatrix by cryptocrystalline silica probably took place during early mesodiagenesis. In turbidite sandstones, such process is commonly driven by silica oversaturation due to the dissolution of radiolaria, diatoms or sponge spicules in the surrounding mudrocks (Sears, 1984; Van Benekon, 1989; Moraes, 1989; Carvalho et al., 1995). In the studied turbidites, it occurred at the bottom of depositional cycles, where mud intraclasts were more common and dissolved silica diffused upward from silica bioclast-rich hemipelagic mudrocks into the sandstones.

During progressive burial, enhanced compaction through intergranular pressure dissolution occurred particularly along contacts with micaceous or carbonaceous grains. This may have played an important role as silica source for quartz overgrowths and grain fracture-healing ingrowths.

Thermobaric mesodiagenesis: salt-dome related reactions

During the thermobaric mesodiagenetic regime (T>100°C), heat and fluid flux related to the adjacent salt domes progressively controlled the evolution of the reservoirs. The convection of hot fluids derived from the underlying mudrocks and limestones with high activities of dissolved Na^+, Ca^{++}, Mg^{++}, Cl^- e $SO4^{--}$ was promoted through the fracture systems around the salt domes.

In salt dome vicinity, shallow-tectonics, halokinesis leads to sandstone fracturing and faulting, which control the distribution of preferential pathways for reactive fluids. During progressive sediment burial, the establishment of thermohaline convection drives diagenetic reactions due to the incremental change of temperature and salinity and to the mass transfer from salt-dome margins (McManus and Hanor, 1988; 1993; Posey and Kyle, 1988; Posey *et al.*, 1994; Esch and Hanor, 1995; Hanor, 1996; Enos and Kyle, 2002; Bruno and Hanor, 2003; Archer et al., 2004).

The main consequence of the action of such hot fluids was the extensive albitization of detrital feldspars, especially of twinned plagioclase and orthoclase grains, whose intensity increases towards the salt domes (**Fig. 13**). The replacement of detrital feldspars by albite occurred associated to the precipitation of albite overgrowths and ingrowths.

Most of quartz overgrowth precipitation also took place under influence of the salt domes, as evidenced by the homogenization temperature and salinity values obtained in fluid inclusions. Salinities are predominantly in the range of 9 to 13 wt% NaCl equivalent, and indicate significant interaction with evaporites.

In most samples, albite and quartz authigenesis were followed by precipitation of blocky dolomite, frequently with saddle habit, and of macrocrystalline late calcite. Isotopic co-variance trend, both for late dolomite and calcite, progressively towards to more negative $\delta^{13}C_{VPDB}$ and $\delta^{18}O_{VPDB}$ values, indicates a genetic derivation from fluids modified by organic matter descarboxylation (**Fig.12**). The authigenesis of albite, quartz and late carbonates were observed in other sandstones associated to salt domes (Land et al., 1987; McManus and Hanor, 1988; 1993; Posey and Kyle, 1988; Burley, 1993; Gaupp et al., 1993; Esch and Hanor, 1995; Giles et al., 2000; Haszeldine et al., 2000; Enos e Kyle, 2002; Archer et al., 2004).

The dissolution of late carbonate cements and garnet grains is probably related to the action of organic acids generated by the thermochemical evolution of kerogen in the underlying mudrocks (Hansley, 1987; Surdam et al., 1989; Hansley e Briggs, 1994; Morton and Hallsworth, 1999). The occurrence of oil inclusions in the quartz overgrowths of some samples indicates that the diagenetic reactions were not interrupted due to initial oil charge. Thermobaric fluids related to oil generation and migration may have contained significant dissolved organic compounds.

Kinetic limitations to thermobaric mesodiagenesis

The occurrence of saddle dolomite, typically associated with coarse pyrite precipitation, has been related to thermochemical sulphate reduction (Machel, 1987, 1989, 2001). Such association seems not to be the case for the studied sandstones, where coarse corrosive mesogenetic pyrite was not identified, despite the availability of sulphate dissolved from the salt domes and of iron from detrital biotite and heavy minerals. Thermochemical sulphate reduction is a process strongly driven by kinetic constraints and occurs mostly within a critical temperature window, presumed to be around 100-140°C (Machel, 2001). Considering that the Urucutuca sandstones have been exposed to temperatures as high as 130–140°C, as documented by microthermometric analysis in fluid inclusions, it seems that the residence time in the critical temperature window was not sufficient to accomplish the process. The present-day temperatures in Cangoá and Peroá fields are 115 and 105°C, respectively.

Illite authigenesis is recognized as a typical mesogenetic process, controlled thermodynamically by changes in mineral stability in response to variation in temperature and fluid chemistry, and kinetically by reaction rates in relation to burial rate, heat and fluid flow (San Juan *et al.*, 2003). Depending on the assumption of the openness and the scale of the diagenetic system, there is an impact on the rising of possible explanations for the source and transport of chemical elements for fibrous illite neoformation in sandstones, which appears to occur mainly due to reaction between kaolinite or smectite and K^+ (Bjørlykke *et al.*, 1986; Ehrenberg and Nadeau, 1989; Chuhan *et al.,* 2000, 2001; Lander and Bonnell, 2010). Potencial sources of potassium would include K-feldspar dissolution within the sandstones (e.g. Bjorlykke *et al.*, 1986, 1992; Bjorkum and Gjelsvik, 1988; Chuhan *et al.*, 2001; Franks and Zwingsmann, 2010) and external sources, such as fluids from associated mudrocks or evaporites (e.g. Gaupp *et al.*, 1993; Robinson *et al.*, 1993; Lanson *et al.*, 1996; Berger *et al.*, 1997; De Ros, 1998; Zwingmann *et al.*, 1999 ; Thyne *et al.*, 2001; Clauer *et al.*, 2008).

Considering these aspects, potassium supply should not have been a constraint for fibrous illite neoformation in Cangoá and Peroá sandstones, as they are feldspar-rich (i.e. internal source), underlain by thick mudrock intervals and surrounded by salt domes (i.e. external sources). However, apart from very scarce transformation of smectitic clay intraclasts (**Fig. 9F**), illite is absent from the sandstones. Moreover, there is no illitization of the abundant kaolinite.

K-feldspar dissolution was common in Cangoá and Peroá reservoirs. Nevertheless, the process was limited to orthoclase grains, while microcline was unaltered, and took place essentially during eodiagenesis related to meteoric influx, what would have leached away K^+ from the sites of feldspar dissolution. On the other hand, considering the availability of K^+ owing to the intense albitization of orthoclase during burial, the absence of illite within the sandstones is intriguing. One possible explanation is that the K^+ released by albitization would preferentially diffuse into the mudrocks or restrictly to mud intraclasts in the sandstone, due to the diffusion gradient generated by smectite illitization, which is energetically favored and requires lower thermal exposure than the neoformation of fibrous illite in the sandstones (Hower *et al.*, 1976; Lander et al., 1990; Stroker and Harris, 2009; Lander and Bonnell, 2010). This argument is supported by XRD analysis. In the < 2um fraction, illite-smectite mixed-layers are volumetrically important in the mudrocks and subordinated in the sandstones, and pure illite is absent in the latter.

Notwithstanding, it is intriguing the coexistence of K-feldspar remnants (mostly microcline, which largely survived meteoric dissolution and burial albitization) with kaolinite at temperatures higher than 100°C, since such association is thermodynamically unstable (Bjorkum and Gjelsvik, 1988), especially considering that the reservoirs were submitted to maximum temperatures as high as 140°C, as indicated by the microthermometry data. In the literature, it is usually documented a marked decline in abundance of kaolinite and K-feldspar reactants at temperatures greater than 120 to 130°C, and that they cease to coexist

at temperatures in excess of 140°C (Bjørlykke *et al.*, 1986; Ehrenberg and Nadeau, 1989; Chuhan *et al.*, 2000, 2001; Franks and Zwingmann, 2010). At temperatures below 100 °C, as suggested by Bjorkum and Gjelsvik (1988), there is a narrow range of conditions where K-feldspar and kaolinite are destabilized to produce authigenic illite. Their theoretical isochemical model is strongly controlled by silica activity in solution. Silica oversaturation would favor their reaction (1) to go to the right, conserving both K-feldspar and kaolinite in equilibrium. If silica is not oversaturated, the reaction would favor illite authigenesis at lower temperatures.

$$KAl_3Si_3O_{10}(OH)_2 + 2SiO_{2\ (aq)} + H_2O \leftrightarrow KAlSi_3O_8 + Al_2Si_2O_5(OH)_4 \qquad (1)$$
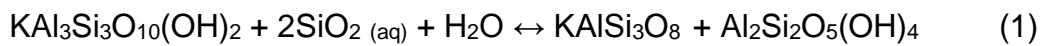
In the studied sandstones, silica oversaturation could have been promoted during meteoric eodiagenesis by the dissolution of silicate grains, and during progressive burial, by the dissolution of biogenic silica in the surrounding mudrocks or by the dissolution of silicate grains due to chemical compaction along intergranular contacts. Moreover, the increasing influence of the salt domes from eodiagenesis to mesodiagenesis, with the consequent increase of salinity and silica solubility, would contribute to maintain silica in solution and stabilize K-feldspar + kaolinite assemblage.

However, even after the exposure to higher temperatures (i.e >100°C), fibrous illite is absent and K-feldspar and kaolinite are still in equilibrium in the reservoirs at the present day. With the aqueous system saturated in silica, the progressive exposure to higher temperatures would overcome kinetic constraints of quartz nucleation and precipitation and, as a consequence, thermodynamically favor illite precipitation.

As dickite is less susceptible to illitization than kaolinite, owing to its better-ordered crystal lattice (Morad *et al.*, 1994; Morad *et al.*, 2000), it could be suggested that the kaolin identified in the studied sandstones be in fact dickite. A pervasive dickitization of kaolinite would

preserve kaolin plus feldspar even at temperatures higher than 100°C (Worden and Morad, 2003). However, this interpretation is not supported by the hydrogen and oxygen isotopic data, which show a close proximity with the meteoric water line, indicating that kaolinite remained stable since it was precipitated.

Other potential sources of K^+ for illite authigenesis in sandstones are formation waters derived from, or influenced by, reactions in associated mudrocks or evaporites. The incursion of potassium-rich brines into the sandstone reservoirs is invoked to explain the precipitation of diagenetic illite in some basins. In an open-system scenario, salt domes are likely to act as a first order control during mesodiagenesis, contributing with energy (thermohaline convection) and mass transfer of solutes to the diagenetic reactions (Hanor, 1996; Hanor, 2001). Transport is a fundamental part of the fluid-rock interaction processes, mainly because it provides the driving force for many of the reactions that take place by continuously introducing fluids out of equilibrium with respect to the reactive solid phases (Steefel and Maher, 2009). Regarding the Peroá and Cangoá reservoirs, as formerly mentioned, the adjacent salt domes served as an important source of Na^+, Mg^{2+} and Ca^{2+}, promoting the precipitation of albite and late carbonates.

We already discussed that smectite illitization in the mudrocks was favored over illite neoformation in the sandstones, because the former reaction requires lower free-energy to occur. This could explain why, even with both internal and external sources of potassium, fibrous illite neoformation has not occurred in the sandstones.

Temperature reached values as high as 140°C in the sandstone reservoirs but such condition likely remained for a short period of time. This may have happened due to the intermittent behavior of faults as hot fluid pathways. Our observation corroborates that illite authigenesis is not simply a universal function of temperature, as stated by Lander and Bonnell (2010). The strong kinetic component of illite neoformation suggests that it is instead

a function of the thermal and fluid recharge history, which controls the illitization temperature range.

Our petrographic and geochemical evidence indicates that neither primary composition, nor pore-water chemistry, nor the temporary exposure to higher temperatures alone were sufficient conditions for illite precipitation in Cangoá and Peroá sandstone reservoirs.

The same argument is proposed to explain the limited quartz cementation of the sandstones. These processes were not energetically favored, owing to the rapid and temporary exposure to higher temperatures and to the late burial of the reservoirs. This contrasts to what have been documented in most reservoirs associated to salt domes as, e.g., in the North Sea Britannia field, offshore Scotland, where quartz cementation had a major impact on reservoir permeability and productivity. Archer *et al.*, (2004) argued that hot and saline diagenetic fluids were focused through a highly permeable zone, radiating away from the Andrew salt dome (10 km to the east), what is consistent with fluid inclusion data and quartz cementation by thick quartz overgrowths with well-developed luminescence zoning. Such conditions never occurred during the evolution of Cangoá and Peroá fields.

There is a clear exploration implication of the diagenetic pattern recognized in Cangoá and Peroá reservoirs. Since that most diagenetic processes promoted by enhanced thermal and fluid flow around salt domes contribute to deteriorate sandstone reservoir porosity and/or permeability, it may be risky to drill too close to salt domes. However, this study shows that the prediction of salt dome-related diagenesis and reservoir quality is rather a function of multiple variables that should include the dimensions of the salt dome itself, the regional thermal regime of the basin, the thermal and fluid conductivity, and the mineral composition and geomechanical properties of the reservoirs and associated lithologies.

CONCLUSIONS

1. The analyzed turbidite sandstones are arkoses, moderately to poorly sorted, immature both texturally and compositionally. Detrital modes obtained through petrographic reconstitution indicate that the source area for the sandstones corresponds to uplifted granitic-gneissic basement rocks.

2. Their diagenetic evolution was influenced by meteoric and marine eogenetic processes and later by the incursion of fluids modified by the interaction with the surrounding evaporites and mudrocks, during the progressive burial of the sequence through mesogenetic compactional and thermobaric stages.

3. Significant dissolution and kaolinization of feldspars, and replacement and expansion of muscovite grains by kaolinite was related to the influx of meteoric water through the turbidite deposits during eodiagenesis, what is corroborated by the $\delta^{18}O$ (+15.3‰ to +18.2‰) and δD (-51‰ to -66‰) isotope signatures obtained in authigenic kaolinite.

4. The deposition of turbidite deposits in the Cangoá Field area was influenced by the salt dome, which acted as physical barrier for the sandy gravitational flows. Halokinesis, still during eogenetic conditions, may have led to an irregular brittle deformation of quartz and feldspar grains. Fracturing of the feldspar grains could have contributed to the increment of reactive surface and favored their dissolution, kaolinization and further albitization. In the Peroá Field, the influence of the salt dome was less pronounced and seems not to have exerted strong control on turbidite deposition.

5. Fluid inclusion data obtained in quartz overgrowths indicate that the turbidite reservoirs were exposed to hot saline fluids (9-13 %wt NaCl and T_h= 105^0–145^0C) during their evolution.

6. Illite was only identified as a product of smectite transformation in the surrounding mudrocks and, very scarcely, of smectitic mud intraclasts in some sandstones. Intergranular fibrous neoformed illite was not identified in the sandstones. This occurred probably because these two reactions are conditioned by distinct thermodynamic and kinetic parameters. The

smectite transformation to illite is energetically favored in relation to the neoformation of fibrous illite.

7. Despite the proximity of the salt domes and the exposure of the reservoirs to high temperature and to saline fluids, the intensity of the diagenetic processes was mild. This is probably related to the short residence time of the reservoirs in such conditions, what have not favored processes highly controlled by chemical kinetics, as illite and quartz authigenesis. The short time in which the reservoirs were exposed to high temperature brines was probably controlled by the intermittent behavior of the faults as conduits for fluid migration.

REFERENCES

Al-Aasm, I.S., Taylor, B.E. and South, B., 1990, Stable isotope analysis of multiple carbonate samples using selective acid extraction: Chemical Geology, 80, 119-125.

Archer, S.G., Wycherley, H.L., Watt, G.R., Baron, M.L., Parnell, J. and Chen, H., 2004, Evidence for focused hot fluid flow within the Britannia field, offshore Scotland, UK: Basin Research, v. 16, No. 3, p. 377-395.

Berger, G., Lacharpagne, J.C., Velde, B., Beaufort, D., and Lanson, B., 1997, Kinetic constraints on illitization reactions and the effects of organic diagenesis in sandstone/shale sequences: Applied Geochemistry, 12, 23-35.

Berner, R., 1978, Rate control of mineral dissolution under Earth surface conditions: American Journal of Science, 278(9), 1235-1252.

Berner, R.A., 1981, Kinetics of weathering and diagenesis, *In* Kinetics of geochemical processes, Lasaga, A.C. and Kirkpatrick, R.J., eds., 8, 111-134.

Berner, R.A., 1984, Sedimentary pyrite formation: an update: Geochimica et Cosmochimica Acta, 48(4), 605-615.

Bigeleisen, J., Perlman, M.L. and Prosser, H.C., 1952, Conversion of hydrogenic materials to hydrogen for stable isotopic analysis: Analytical Chemistry, 24, p. 1356-1357.

Bjørkum, P.A., and Gjelsvik, N., 1988, An isochemical model for formation of authigenic kaolinite, K-feldspar and illite in sediments: Journal of Sedimentary Research, 58, 506-511.

Bjørlykke, K., Aagaard, P., Dypvik, H., Hastings, D.S., and Harper, A.S., 1986, Diagenesis and reservoir properties of Jurassic sandstones from the Haltenbanken area, offshore mid-Norway, *In* Habitat of hydrocarbons on the Norwegian continental shelf, Spencer, A.M. *et al.*, eds., Nor.Petr.Soc., 275-286.

Bjørlykke, K., and Aagaard, P., 1992, Clay minerals in North Sea sandstones, *in* Houseknecht, D.W. and Pittman, E.D., eds., Origin, Diagenesis, and Petrophysics of Clay Minerals in Sandstones, SEPM Special Publication 47, p. 65-80.

Bjørlykke, K., Nedkvitne, T., Ramm, M., and Saigal, G., 1992, Diagenetic processes in the Brent Group (Middle Jurassic) reservoirs of the North sea – an overview, *In* Geology of the Brent Group, Morton, A.C. *et al.*, eds., Geological Society of London Special Publication 61, 263-287.

Bruhn, C.H.L., 2001. Contrasting types of Oligocene/Miocene giant turbidite reservoirs from deep water Campos Basin, Brazil. *In*: AAPG Distinguished Lecture.

Burley, S.D., 1993, Models of burial diagenesis for deep exploration plays in Jurassic fault traps of the Central and Northern North Sea, *in* Parker, J.R., ed., Petroleum Geology of Northwest Europe: Proceedings of the 4th Conference: London, UK, The Geological Society, p. 1353-1375.

Bruno, R.S. and Hanor, J.S., 2003, Large-scale fluid migration driven by salt dissolution, Bay Marchand Dome, offshore Louisiana: GCAGS Transactions, v. 53, p. 97-107.

Carvalho, R.S., 1989, Bacia do Espírito Santo: o "estado da arte" da exploração: I Sintex – Seminário de Interpretação Exploratória, 127-134.

Carvalho, M.V.F., De Ros, L.F., Gomes, N.S., 1995, Carbonate cementation patterns and diagenetic reservoir facies in the Campos Basin Cretaceous turbidites, offshore eastern Brazil: Marine and Petroleum Geology, 12, 741-758.

Choquette, P.W. and Pray, L.C., 1970, Geologic nomenclature and classification of porosity in sedimentary carbonates: AAPG Bulletin, v. 54/2, p. 207-244.

Chuhan, F., Bjorlykke, K., Lowrey, C., 2000, The role of provenance in illitization of deeply buried reservoir sandstones from Haltenbanken and north Viking Graben, offshore Norway: Marine and Petroleum Geology, 17, 673-689.

Chuhan, F., Bjorlykke, K., Lowrey, C., 2001, Closed system burial diagenesis in reservoir sandstones: Examples from the Garn Formation at Haltenbanken area, offshore mid-Norway: Journal of Sedimentary Research, 71, 15-26.

Clauer, N., Liewig, N., Ledesert, B., and Zwingmann, H., 2008, Thermal history of Triassic sandstones from the Vosges Mountains-Rhine Graben rifting area, NE France, based on K-Ar illite dating: Clay Minerals, 43, 363-379.

Clayton, R.N. and Mayeda, T.K., 1963, The use of bromine pentafluoride in the extraction of oxygen from oxides and silicates for isotopic analysis: Geochimica Cosmochimica Acta, 27, 43-52.

Cordani, U.G. and Blazekovic, A., 1970, Idades radiométricas das rochas vulcânicas de Abrolhos, *in* Anais XXIV Congresso Brasileiro de Geologia, v.1, Porto Alegre, 265-270.

Del Rey, A.C. and Zembruscky, S.G., 1991, Estudo hidrogeotérmico das bacias do Espírito Santo e Mucuri: Boletim de Geociências da PETROBRAS, 5, 25-38.

Deming, D., and Nunn, J.A., 1991, Numerical simulations of brine migration by topographically driven recharge: Journal of Geophysical Research, 96(B2), 2485-2499.

De Ros, L.F., 1998, Heterogeneous generation and evolution of diagenetic quartz arenites in the Silurian-Devonian Furnas Formation of the Paraná Basin, southern Brazil: Sedimentary Geology, 116, 99-128.

Dickinson, W.R., 1985, Interpreting provenance relations from detrital modes of sandstones. In: Provenance of Arenites: Zuffa, G. G. (Ed.), NATO-ASI Series C, v. 148: Dordercht, The Netherlands, D. Reidel Pub. Co., p. 333-361.

Dutton, S., 2008, Calcite cement in Permian deep-water sandstones, Delaware basin, west Texas: origin, distribution and effect on reservoir properties: AAPG Bulletin, 92, 765-787.

Ehrenberg, S.N., and Nadeau, P.H., 1989, Formation of diagenetic illite in sandstones of the Garn Formation, Haltenbanken area, mid-Norweigien continental shelf: Clay Minerals, 24, 233-253.

Empinotti, T.C., Paraízo, P., Moraes, M.A.S., Oliveira, T., 2011. An integrated approach for the study of deep-water reservoirs. AAPG ICE, Milan, Italy, October 2011. AAPG Search and Discovery Article #90135.

Enos, J.S. and Kyle, J.R., 2002, Diagenesis of the Carrizo sandstone at Butler salt dome, East Texas Basin, U.S.A.: Evidence for fluid-sediment interaction near halokinetic structures: Journal of Sedimentary Research, v. 72, p. 68-81.

Esch, W.L. and Hanor, J.S., 1995, Fault and fracture control of fluid and diagenesis around the Iberia salt dome, Iberia Parish, Louisiana: GCAGS Transactions, v. 45, p. 31-45.

Estrella, G., Mello, M.R., Gaglianone, P.C., Azevedo, R.L.M., Tsubone, K., Rossetti, E., Concha, J., Brüning, I.M.R.A., 1984, The Espírito Santo Basin, Brazil: source rock characterization and petroleum habitat, *in* Demaison, G. and Murris, R.J., eds., Petroleum Geochemistry and Basin Evaluation: AAPG Memoir, American Association of Petroleum Geologists, Tulsa, Oklahoma, p. 253-271.

Fetter, M., De Ros, L.F. and Bruhn, C.H.L., 2009, Petrographic and seismic evidence for the depositional setting of giant turbidite reservoirs and the paleogeographic evolution of Campos Basin, offshore Brazil: Marine and Petroleum Geology, 26, 824-853.

Folk, R.L., 1968, Petrology of Sedimentary Rocks. Austin, Texas, Hemphill`s, 107 p.

Franks, S.G., and Zwingmann, H., 2010, Origin and timing of late diagenetic illite in the Permian-Carboniferous Unayzah sandstone reservoirs of Saudi Arabia: AAPG Bulletin, 94, 1133-1159.

Friedman, G.M., 1959, Identification of carbonate minerals by staining methods: Journal of Sedimentary Petrology, v.29, No.1, 87-97.

Friedman, I. and O'Neil, J.R., 1977, Compilation of stable isotopic fractionation factors of geochemical interest, *in* Fleischer, M., ed., Data of Geochemistry, 6th Ed. USGS Professional Paper. United States Geological Survey, p.12.

Gallagher, K., Hawkesworth, C.J., and Mantovani, M.S.M., 1995, Denudation, fission track analysis and the long-term evolution of passive margin topography: Application to the southeast Brazilian margin: Journal of South American Earth Science, 8, 65-77.

Gallagher, K., and Brown, R., 1999, The Mesozoic denudation history of the Atlantic margins of southern Africa and southeast Brazil and the relationship to offshore sedimentation, *In* The oil and gas habitats of the South Atlantic, Cameron, N.R., Bate, R.H., and Clure, V.S., eds., Geological Society of London Special Publication, 41-53.

Galloway, W. E., 1984, Hydrogeologic regimes of sandstone diagenesis, in D. A. McDonald, and R. C. Surdam, eds., Clastic Diagenesis: AAPG Memoir 37, p. 3–14.

Gaupp, R., Matter, A., Platt, J., Ramseyer, K. and Walzebuck, J., 1993, Diagenesis and fluid evolution of deeply buried Permian (Rotliegende) gas reservoirs, northwest Germany: AAPG Bulletin, 77, 1111-1128.

Giles, M.R., Indrelid, S.L., Beynon, G.V., and Amthor, J., 2000, The origin of large-scale quartz cementation: evidence from large data sets and coupled heat- fluid mass

transport modelling, *in* Worden, R.H. and Morad, S., eds., Quartz Cementation in Sandstones: IAS Special Publication, v. 29, 21-38.

Hanor, J.S., 1996, Variations in chloride as a driving force in siliciclastic diagenesis, *In* Siliciclastic diagenesis and fluid flow: concepts and applications, SEPM Special Publications 55.

Hanor, J.S., 2001, Reactive transport involving rock-buffered fluids of varying salinity: Geochimica et Cosmochimica Acta, 65 (21), 3721-3732.

Hansley, P.L., 1987, Petrologic and experimental evidence for the etching of garnets by organic acids in the Upper Jurassic Morrison Formation, northwestern New Mexico. Journal of Sedimentary Petrology, 57, 4, p. 666-681.

Hansley, P.L., and Briggs, P.H., 1994, Garnet dissolution in oxalic acid – A possible analog for natural etching of garnet by dissolved organic matter: USGS Bulletin 2106.

Haszeldine, R.S., Macaulay, C.I., Marchand, A., 2000, Sandstone cementation and fluids in hydrocarbon basins: Journal Geochemical Exploration, 69-70, 195-200.

Hower, J., Eslinger, E.V., Hower, M.E., and Perry, E.A., 1976, Mechanism of burial metamorphism of argillaceous sediment: 1. Mineralogical and chemical evidence: Geological Society of America Bulletin, 87, 725-737.

Ketzer, J.M., Morad, S., and Amorosi, A., 2003, Predictive diagenetic clay mineral distribution in siliciclastic rocks within a sequence stratigraphic framework, *In* Worden, R.H., and Morad, S., eds., Clay mineral cements in sandstones, IAS Special Publication, 34, 43-61.

Land, L., Milliken, K.L., and McBride, E.F., 1987, Diagenetic evolution of Cenozoic sandstones, Gulf of Mexico sedimentary basin: Sedimentary Geology, 50, 195-225.

Lander, R.H., Bloch, S., Mehta, S., and Atkinson, C.D., 1990, Burial diagenesis of paleosols in the Giant Yacheng Gas field, People's Republic of China: bearing on illite reaction pathways: Journal of Sedimentary Research, 61, 256-268.

Lander, R.H., and Bonnell, L.M., 2010, A model for fibrous illite nucleation and growth in sandstones: AAPG Bulletin, 94, 1161-1187.

Lanson, B., Beaufort, D., Berger, G., Baradat, J., and Lacharpagne, J.C., 1996, Illitization of diagenetic kaolinite-to-dickite conversion series: Late-stage diagenesis of the Lower Permian Rotliegende sandstone reservoir, offshore of the Netherlands: Journal of Sedimentary Research, 66, 501-518.

Machel, H.G., 1987, Some aspects of diagenetic sulphate-hydrocarbon redox reactions, *in* Marshall, J.D., ed., Diagenesis of Sedimentary Sequences: Geological Society Special Publication, n. 36, pp. 15-28.

Machel, H.G., 1989, Relationships between sulphate reduction and oxidation of organic compounds to carbonate diagenesis, hydrocarbon accumulations, salt domes and metal sulphide deposits: Carbonate and Evaporites, 4, 137-151.

Machel, H.G., 2001, Bacterial and thermochemical sulfate reduction in diagenetic settings - old and new insights: Sedimentary Geology, v. 140, p. 143-175.

Mansurbeg, H., El-ghali, M.A.K., Morad, S., Plink-Björklund, P., 2006, The impact of meteoric water on the diagenetic alterations in deep-water, marine siliciclastic turbidites: Journal of Geochemical Exploration, 89 (1-3), 254-258.

Mansurbeg, H., Morad, S., Salem, A., Marfil, R., El-Ghali, M.A.K., Nystuen, J.P., Caja, M.A., Amorosi, A., Garcia, D., And La Iglesia, A., 2008, Diagenesis and reservoir quality evolution of Palaeocene deepwater, marine sandstones, the Shetland-Faroes Basin, the British continental shelf: Marine and Petroleum Geology, 25, 514–543.

Mansurbeg, H., De Ros, L.F., Morad, S., Ketzer, J.M., El-ghali, M.A.K., Caja, M.A., Othman, R., 2012, Meteoric-water diagenesis in late Cretaceous canyon-fill turbidite reservoirs from the Espírito Santo basin, eastern Brazil: Marine and Petroleum Geology, 37, 7-26.

Makowitz, A., and Milliken, K.L., 2003, Quantification of brittle deformation in burial compaction, Frio and Mount Simon Formation sandstones: Journal of Sedimentary Research, 73(6), 1007-1021.

McManus, K.M., and Hanor, J.S., 1988, Calcite and iron sulfide cementation of Miocene sediments flanking the West Hackberry salt dome, southwest Louisiana, U.S.A: Chemical Geology, v. 74, No. 1-2, Fluid-Rock Interactions in the Salt Dome Environment, p. 99-112.

McManus, K.M., and Hanor, J.S., 1993, Diagenetic evidence for massive evaporite dissolution, fluid flow, and mass transfer in the Louisiana Gulf Coast: Geology, v. 21, p. 727–730.

Milliken, K., and Laubach, S., 2000, Brittle deformation in sandstone diagenesis as revealed by scanned cathodoluminescence imaging with application to characterization of fractured reservoirs, *In* Cathodoluminescence in Geosciences, Pagel, M., Barbin, V., Blanc, P., Ohnenstetter, D., eds., Springer:Berlin, 225-243.

Morad, S., 1986, Albitization of K-feldspar grains in Proterozoic arkoses and greywackes from southern Sweden: N. Jb. Miner. Mh., 4, 145-156.

Morad, S., Bergan, M., Knarud, R., and Nystuen, J.P., 1990, Albitization of detrital plagioclase in Triassic reservoir sandstones from the Snorre Field, Norwegian North Sea: Journal of Sedimentary Research, 60, 411-425.

Morad, S., Ben Ismail, H., De Ros, L.F., Al-Aasm, I.S., and Serrhini, N.-E., 1994, Diagenesis and formation water chemistry of Triassic reservoir sandstone from southern Tunisia: Sedimentology, 41, 1253-1272.

Morad, S., 1998, Carbonate cementation in sandstones: distribution patterns and geochemical evolution, *In* Carbonate Cementation in Sandstones: distribution patterns and geochemical evolution, Morad, S., ed., IAS Special Publication vol. 26, 1-26.

Morad, S., Ketzer, J.M., and De Ros, L.F., 2000, Spatial and temporal distribution of diagenetic alterations in siliciclastic rocks: implications for mass transfer in sedimentary basins: Sedimentology, 47, 95-120.

Morad, S., Worden, R.H., and Ketzer, J.M., 2003, Oxygen and hydrogen isotopic composition of diagenetic clay minerals in sandstones: a review of the data and controls, *In* Clay minerals cements in sandstones, Worden, R.H. and Morad, S., eds., IAS Special Publication, 34, 63-92.

Morad, S., Al-Ramadan, K., Ketzer, J.M., De Ros, L.F., 2010, The impact of diagenesis on the heterogeneity of sandstone reservoirs: A review of the role of depositional facies and sequence stratigraphy: AAPG Bulletin, 94, 1267-1309.

Moraes, M., 1989, Diagenetic evolution of Cretaceous-Tertiary turbidite reservoirs, Campos Basin, Brazil: AAPG Bulletin, 73, 598-612.

Morton, A.C. and Hallsworth, C.R., 1999, Processes controlling the composition of heavy mineral assemblages in sandstones. Sedimentary Geology, v. 124, Nos. 1–4, p. 3-29.

Posey, H.H., and Kyle, J.R., 1988, Fluid-rock interactions in the salt dome environment: an introduction and review: Chemical Geology, v. 74, No. 1-2, Fluid-Rock Interactions in the Salt Dome Environment, p. 1-24.

Posey, H.H., Kyle, J.R., and Agee Jr., W.N., 1994, Relations between diapiric salt structures and metal concentrations, Gulf Coast sedimentary basin, southern North America, *in* Fontbote, L., and Boni, M., eds., Sediment-hosted Zn–Pb Ores: Berlin, Springer-Verlag, 139–164.

Prochnow, E.A., Remus, M.V.D., Ketzer, J.M., Gouvea Jr., J.C.R., Schiffer, R. and De Ros, L.F., 2006, Organic-inorganic interactions in oilfield sandstones: examples from turbidite reservoirs in the Campos basin, offshore eastern Brazil: Journal of Petroleum Geology, 29, 361-380.

Reed, R.M., and Laubach, S.E., 1996, The role of microfractures in the development of quartz overgrowth cements in sandstones: new evidence from cathodoluminescence studies: Geological Society of America Annual Meeting, 28 (7), 280.

Robinson, A.G., Coleman, M.L., Gluyas, J.G., 1993, The age of illite cement growth, Village fields area, southern North Sea: Evidence from K-Ar ages and $^{18}O/^{16}O$ ratios: AAPG Bulletin, 77, 68-80.

Rosenbaum, J.M. and Sheppard, S.M.F., 1986, An isotopic study of siderites, dolomites and ankerites at high temperatures: Geochimica Cosmochimica Acta, 50, 1147-1150.

Saigal, G.C., Morad, S., Bjørlykke, K., Egeberg, P.K. and Aagaard, P., 1988, Diagenetic albitization of detrital K-feldspars in Jurassic, Lower Cretaceous, and Tertiary clastic reservoirs from offshore Norway, I. Textures and origin: Journal of Sedimentary Research, 58, 1003-1013.

SanJuan, B., Girard, J.P., Lanini, S., Bourguignon, Brosse, E., 2003, Geochemical modelling of diagenetic illite and quartz cement formation in Brent sandstone reservoirs: example of the Hild Field, Norwegian North Sea, *In* Clay minerals cements in sandstones, Worden, R. and Morad, S., eds., IAS Special Publication, n. 34, 425-452.

Savin, S.M., and Epstein, S., 1970, The oxygen and hydrogen isotope geochemistry of clay minerals: Geochimica et Cosmochimica Acta, 34, 25-42.

Schmidt, V., and McDonald, D.A., 1979, The role of secondary porosity in the course of sandstone diagenesis, *in* Scholle, P.A. and Schluger, P.R., eds., Aspects of Diagenesis, SEPM Special Publication 29, Society of Economic Paleontologists and Mineralogists, Tulsa, Oklahoma, p. 175-207.

Sears, S.O., 1984, Porcellaneous cement and microporosity in California Miocene turbidites – origin and effect on reservoir properties: Journal of Sedimentary Research, 54, 159-169.

Sheppard, S.M.F., and Gilg, H.A., 1996, Stable isotope geochemistry of clays: Clay Mineral, 31, 1-24.

Steefel, C., and Maher, K., 2009, Fluid-Rock Interaction: A Reactive Transport Approach, *In* Reviews in Mineralogy & Geochemistry, Mineralogical Society of America, vol. 70, 485-532.

Stroker, T., and Harris, N., 2009, K-Ar dating of authigenic illites: Integrating diagenetic history of the Mesa Verde Group, Piceance Basin, NW Colorado (abs.): AAPG Annual Meeting Abstracts, 18, 206.

Surdam, R.C., Boese, S.W., Crossey, L.J., 1984, The chemistry of secondary porosity, *In* Clastic Diagenesis, McDonald, D.A. and Surdam, R.C., eds., AAPG Memoir, 37, 127-149.

Surdam, R.C., Dunn, T.L., Heasler, H.P., and MacGowan, D.B., 1989, Porosity evolution in sandstone/shale systems, *in* Hutcheon, I.E., ed., Short Course on Burial Diagenesis: Mineralogical Association of Canada Short Course Handbook, v. 15, p. 61–133.

Tello Saenz, C.A.T., Hackspacher, P.C., Neto, J.C.H., Iunes, P.J., Guedes, S., Ribeiro, L.F.B., and Paulo, S.R., 2003, Recognition of Cretaceous, Paleocene and Neogene tectonic reactivation through apatite fission-track analysis in Precambrian areas of southeast Brazil: association with the opening of the South-Atlantic Ocean: Journal of South American Earth Science, 15(7), 765-774.

Tello Saenz, C.A.T., Hadler Neto, J.C., Iunes, P.J., Guedes, S., Hackspacher, P.C., Ribeiro, L.F.B., Paulo, S.R., Osorio, A.M., 2005, Thermochrology of the South American platform in the state of São Paulo, Brazil, through apatite fission tracks: Radiat. Meas., 39, 635-640.

Thyne, G., Boudreau, B.P., Ramm, M., and Midtbo, R.E., 2001, Simulation of potassium feldspar dissolution and illitization in the Statfjord Formation, North Sea: AAPG Bulletin, 85, 621-635.

Van Benekkon, A.J., Jansen, J.H., Van der Gaast, S.J., Van Peren, J.M., and Pieters, J., 1989, Aluminium-rich opal: an intermediate in the preservation of biogenic silica in the Zaire (Congo) deep-sea fan: Deep-Sea Research, 36, 173-190.

Vennemann, T.W. and O'Neil, J.R., 1993, A simple and inexpensive method of hydrogen isotope and water analyses of minerals and rocks based on zinc reagent: Chemical Geology, 103, 227-234.

Vieira, P.E., Biassusi, A.S., Brandão, J.R., 1999, Arcabouço preditivo de fácies arenosas no Terciário *offshore* da Bacia do Espírito Santo. In: SIMPÓSIO SOBRE TURBIDITOS, 2, Rio de Janeiro, 1999. Boletim de Resumos Expandidos. Rio de Janeiro: PETROBRAS/SEREC/CEN-SUD, 66-70.

Wilson, M.D. and Stanton, P.T., 1994, Diagenetic mechanisms of porosity and permeability reduction and enhancement, *in* Reservoir Quality Assesment and Prediction in Clastic Rocks, SEPM Short Course Notes, v.30, p. 59-117.

Worden, R. and Morad, S., 2003, Clay minerals in sandstones: controls on formation, distribution and evolution, *In* Clay minerals cements in sandstones, Worden, R. and Morad, S., eds., IAS Special Publication, n. 34, 3-42.

Zwingmann, H., Clauer, N., Gaupp, R., 1999, Structural related geochemical (REE) and isotopic characteristics (K-Ar, Rb-Sr, del[18]O) characteristics of clay minerals from Rotliegende sandstone reservoirs (Permian, northern Germany): Geochimica et Cosmochimica Acta, v. 63, 2805-2823.
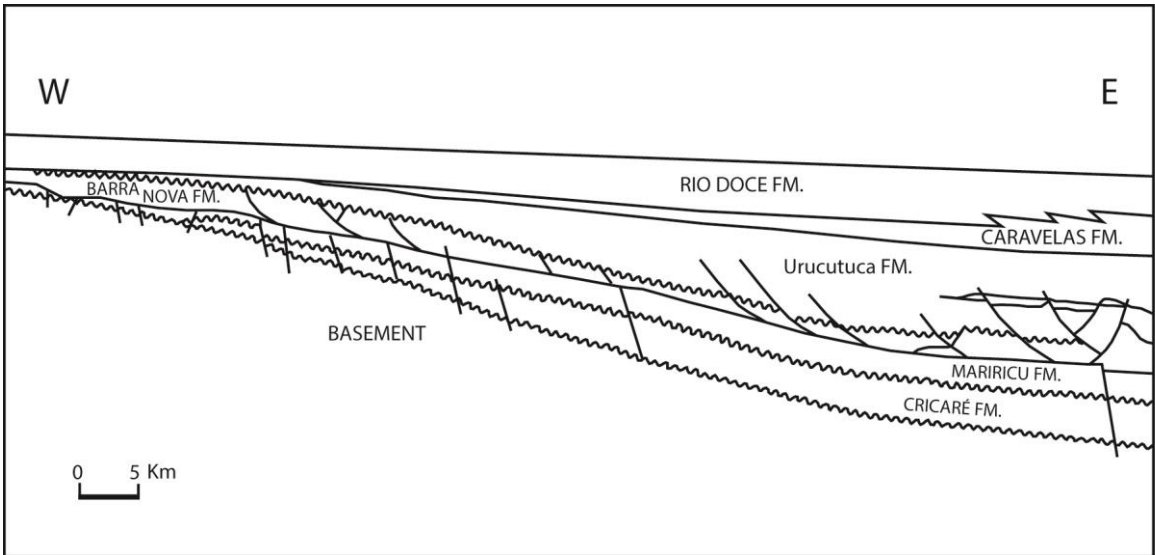
Figure 1. A schematic dip section of the basin showing the thickening of the Urucutuca Formation towards east (modified after Del Rey and Zembruscky, 1991).
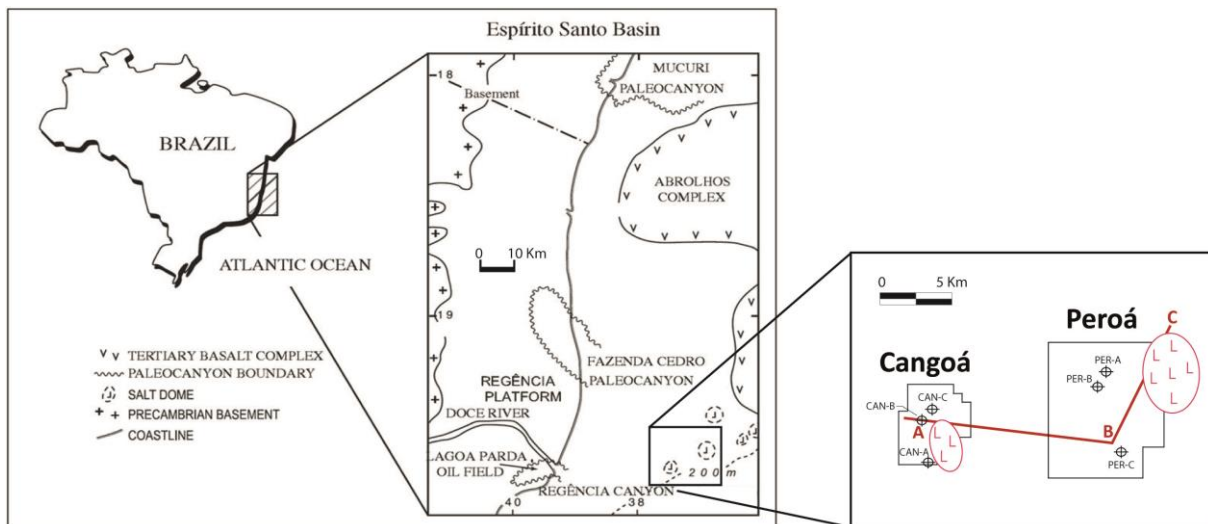
Figure 2. Location map of the studied area in the Espírito Santo Basin. The detail indicates the location of Cangoá and Peroá oilfields and the sections presented in Figure 3.
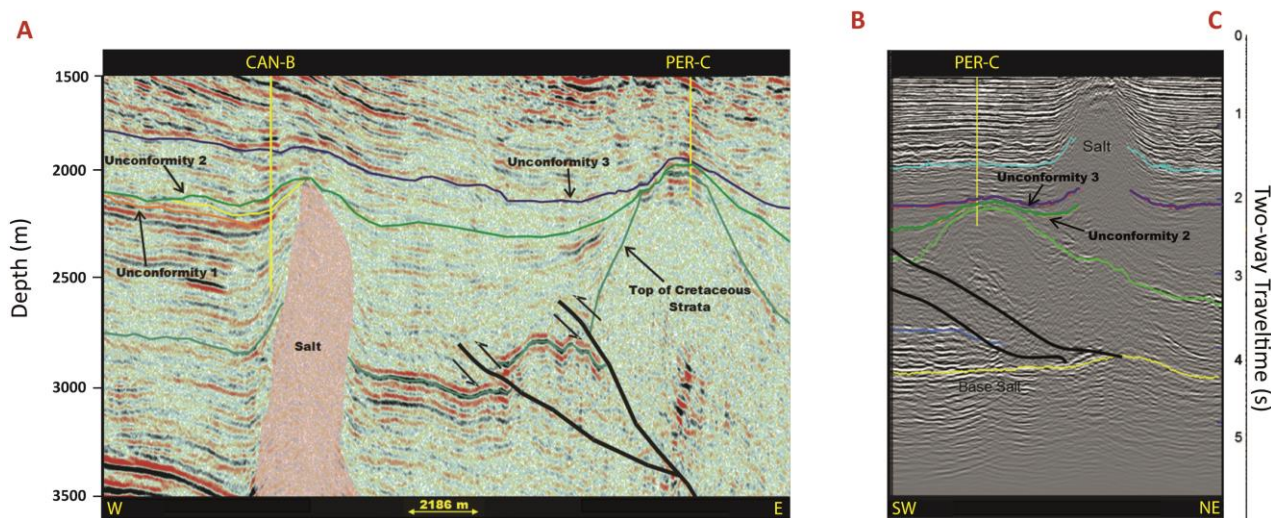

Figure 3. Seismic sections indicated in Figure 2, showing the structural context of Cangoá and Peroá oilfields. Reservoir intervals are both limited at bottom and top by regional unconformities. A thick thrusted wedge of cretaceous mudrocks is a prominent structural feature of the Peroá area. Note that the vertical scale presented in B-C section is in two-way traveltime seconds.
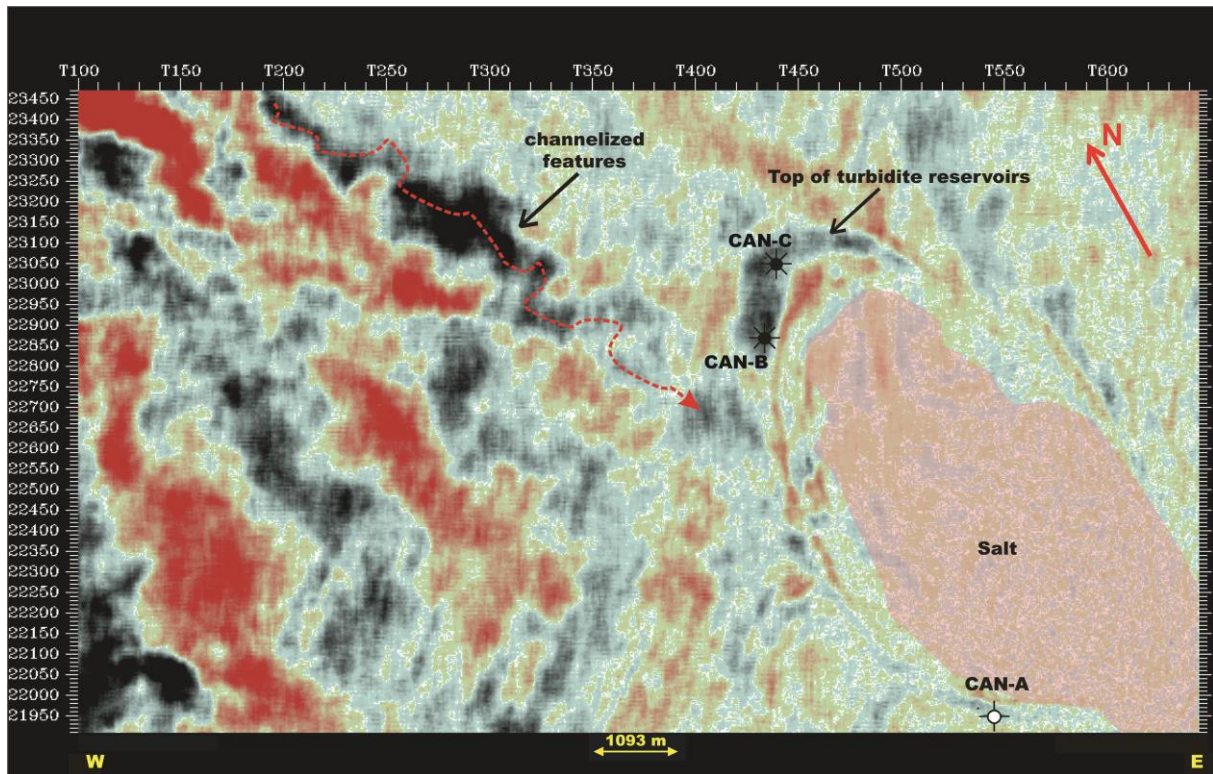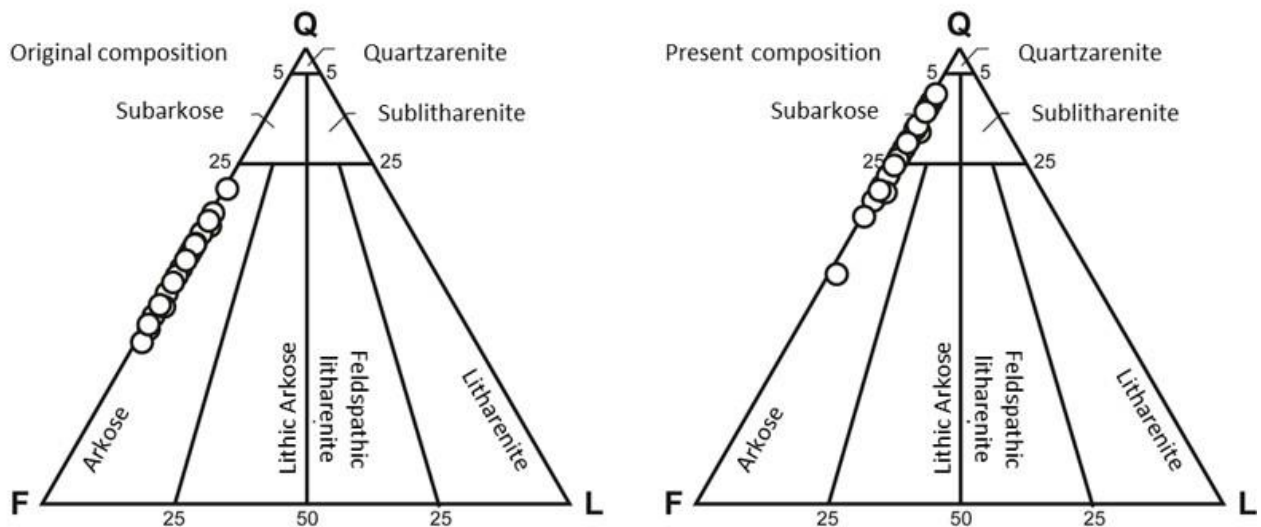
Figure 4. A time slice seismic image revealing the northwestern flank of Cangoá salt dome, where the Eocene turbidite reservoirs are located. Note the concentric fractures system affecting the surrounding sandstones and mudrocks.
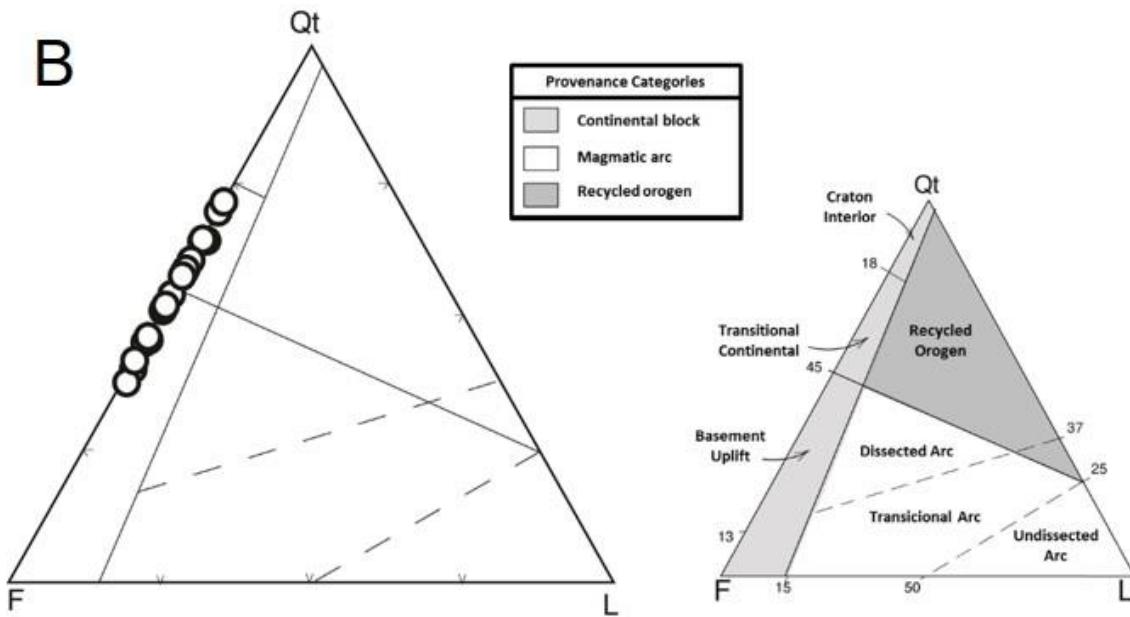
Figure 5. (A) Original and present detrital composition of the studied sandstones plotted on Folk (1968) classification diagram. (B) Essential original composition of the studied sandstones plotted on Dickinson (1985) tectonic provenance diagram.
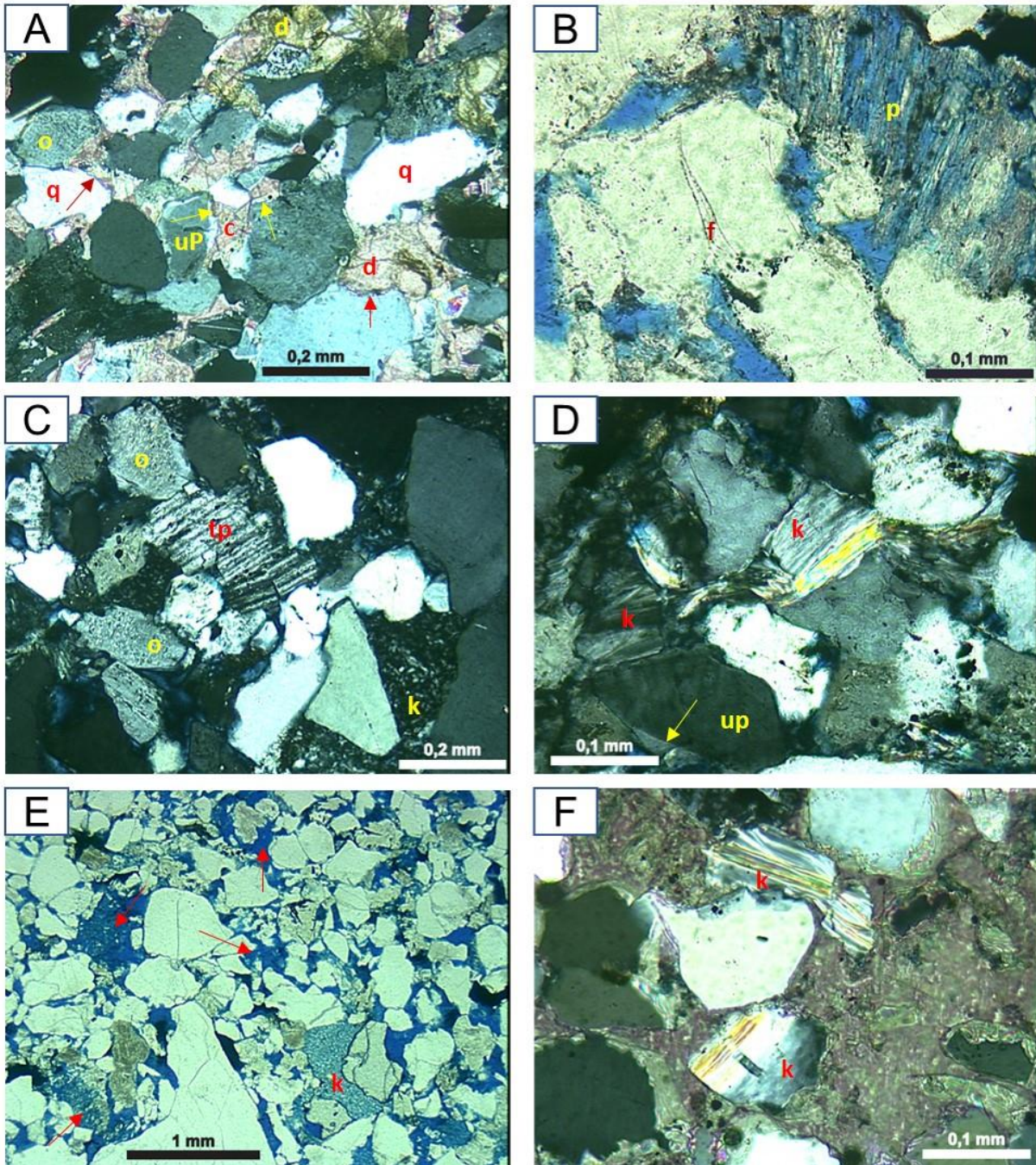
Figure 6. A) Late calcite (c) and dolomite (d) covering and replacing albite and quartz overgrowths (arrows). Ortoclase grains fully albitized (o) and untwinned plagioclase (uP) covered by albite overgrowth. Crossed polarizers (XP). CAN-A 3316,15. B) Feldspar grain partially dissolved and albitized (p). Quartz grain fractured and "healed" by quartz ingrowth (f). Uncrossed polarizers (//P). CAN-C 3093,6. C) Twinned plagioclase grain fractured and "healed" by albitization (tp). Albitized orthoclase grains covered by albite overgrowths. Intergranular kaolinite. XP. CAN-B 3062,25. D) Lamellar kaolinite replacing and expanding mica grains (k). Untwinned plagioclase (up) covered by albite overgrowth (arrow). XP. CAN-C 3086,2. E) Porous sandstone with intragranular pores due to the dissolution of feldspar grains (arrows). Booklet aggregates of kaolinite replacing feldspar grains (k). //P. CAN-A 3163,1. F) Pre-compactional poikilotopic calcite (stained pink) cementing and replacing grains. Note that calcite cementation post-dates mica expansion (k). XP. PER-A 2814,75.
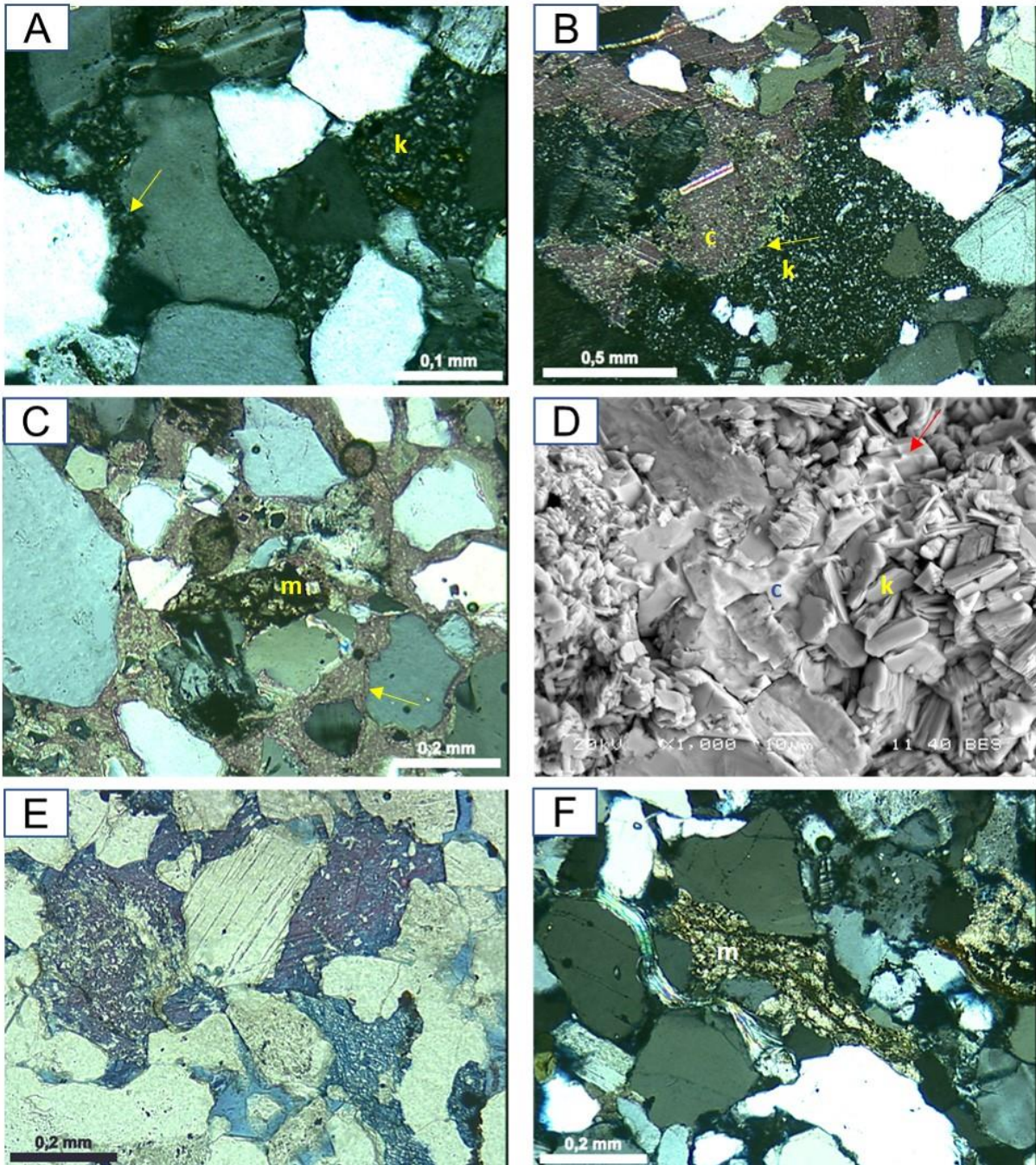
Figure 7. A) Aggregates of kaolinite with microcrystalline and booklet habits filling intergranular porosity and locally engulfed by quartz overgrowths (arrow). XP. CAN-B 3078,7. B) Pre-compactional poikilotopic calcite (c) replacing grains and authigenic kaolinite (k) (arrow). XP. CAN-B 3082,6. C) Pre-compactional poikilotopic calcite cementing grain (m) previously replaced by microcrystalline pyrite and dolomite (probable biotite) and marginally corroding grains (arrow). XP. PER-A 2814,75. D) Scanning electron micrograph of calcite cement (c) engulfing and replacing aggregates of kaolin platelets (k). E) Ferroan calcite (stained violet) cementing and replacing framework grains and ferroan dolomite (stained blue). Uncrossed polarizers (//P). CAN-B 3062,25. F) Pre-compactional microcrystalline dolomite and pyrite replacing and expanding biotite lamellae (m). XP. PER-A 2816,8.
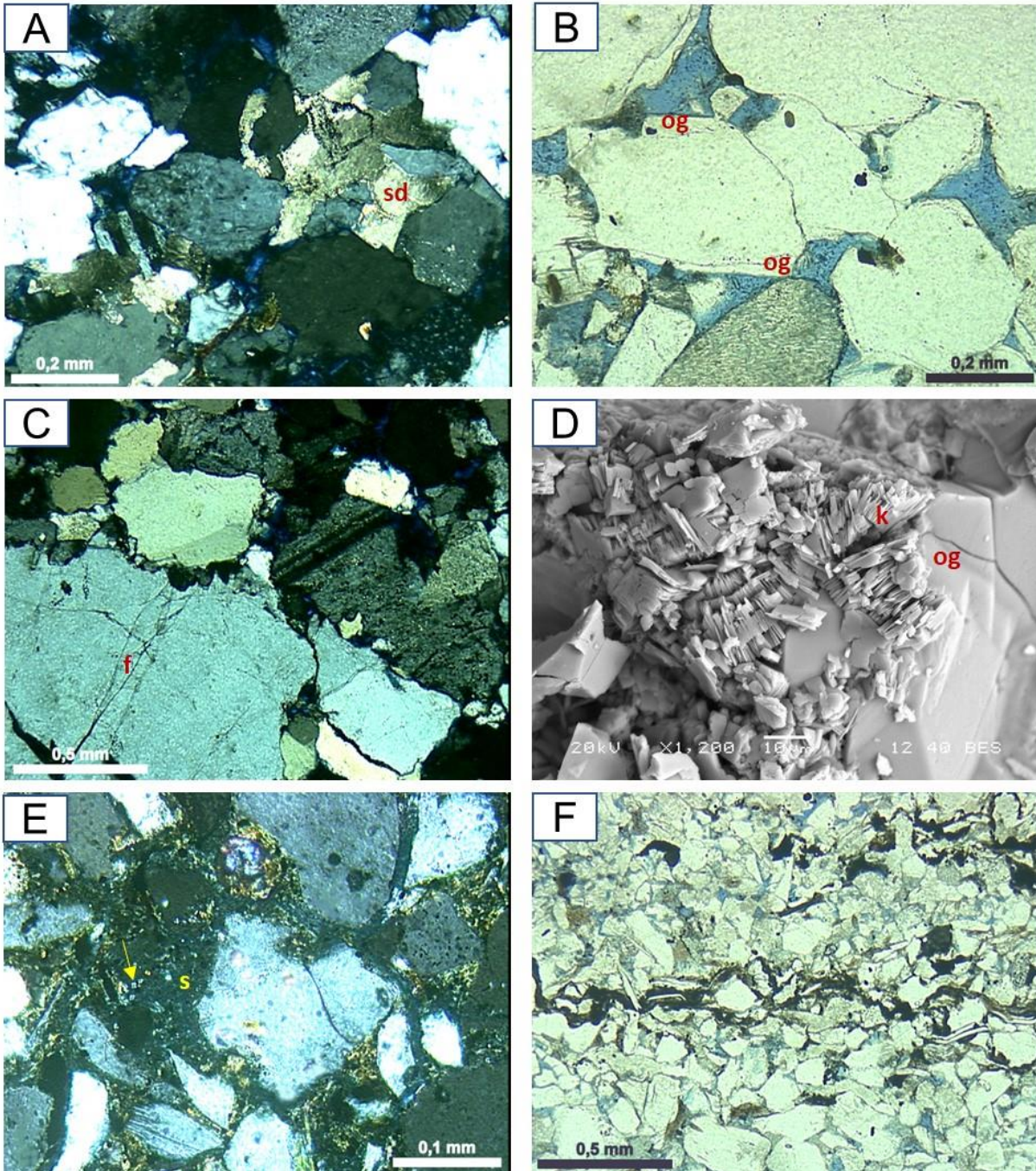
Figure 8. A) Saddle dolomite crystals (sd) with wavy extinction cementing and marginally replacing framework grains. XP. CAN-C 3095,45. B) Discontinuous quartz overgrowths (og). //P. CAN-B 3082,6. C) Fractured quartz grains "healed" by quartz ingrowths (f) and affected by intergranular pressure dissolution. XP. CAN-C 3076,55. D) Scanning electron micrograph displaying kaolin platelets (k) engulfed by quartz overgrowth (og). E) Mud intraclasts with nannnofossils (arrow) and derived pseudomatrix replaced by cryptocrystalline silica (s). XP. PER-C-ESS 2680,45. F) Stylolitic surfaces locally developed along intervals enriched in mica grains and carbonaceous fragments. //P. CAN-B 3078,70.
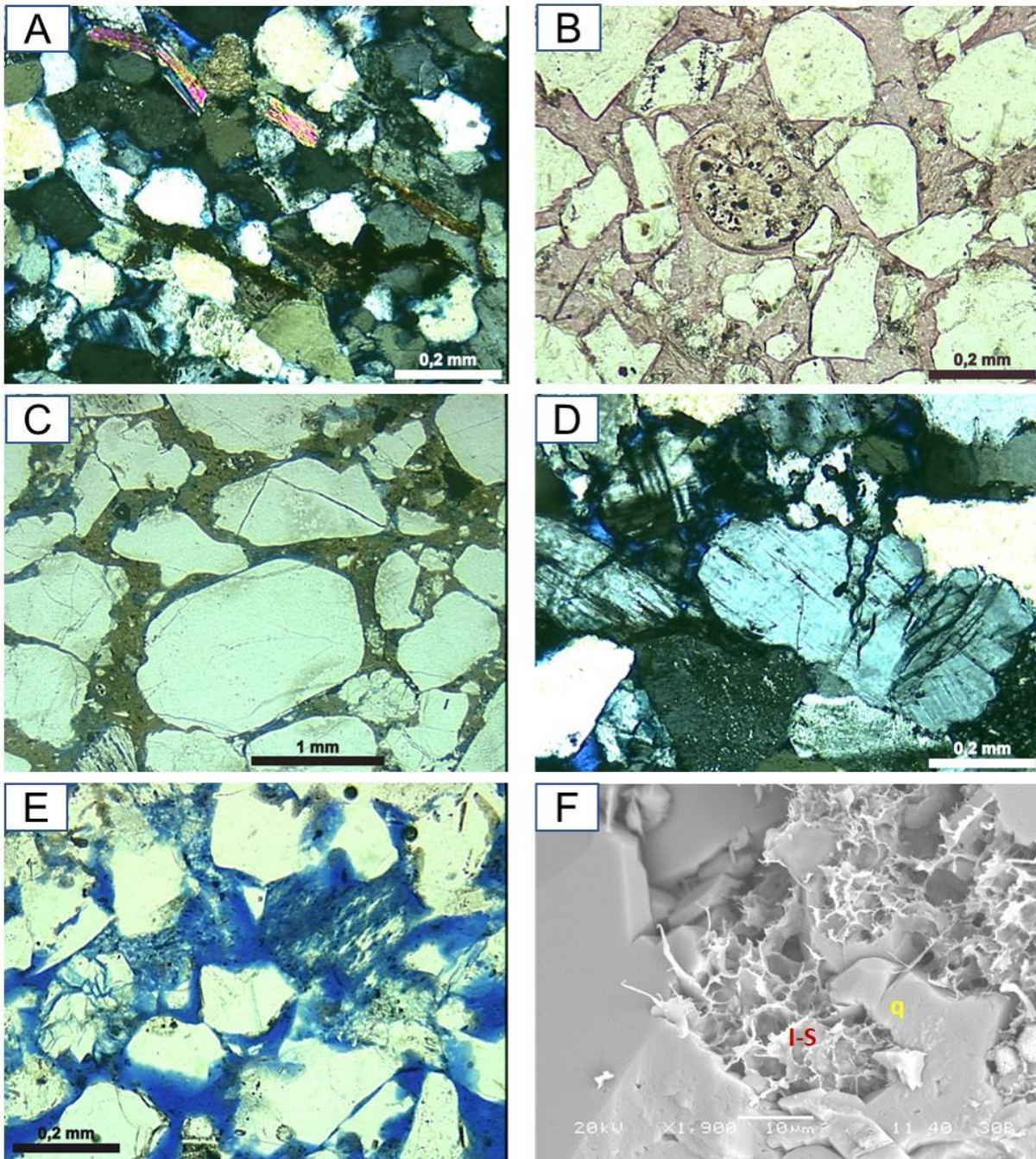
Figure 9. A) Mica-rich sandstone with abundant biotite (partially pyritized) and muscovite grains. XP. CAN-C 3086,2. B) Sandstone pervasively cemented by poikilotopic calcite (stained pink). Foraminifer bioclast partially filled with framboidal pyrite. //P. CAN-C 3081,45. C) Mud pseudomatrix from the compaction of intraclasts. //P. CAN-B 3080,5. D) Fractured feldspar grains. XP. CAN-C 3093,6. E) Enhanced dissolution of feldspars in interval affected by grain fracturing. //P. PER-A 3016,6. F) Scanning electron micrograph of smectite-illite mixed layer (I-S) (mud pseudomatrix) engulfed by quartz overgrowth (q).

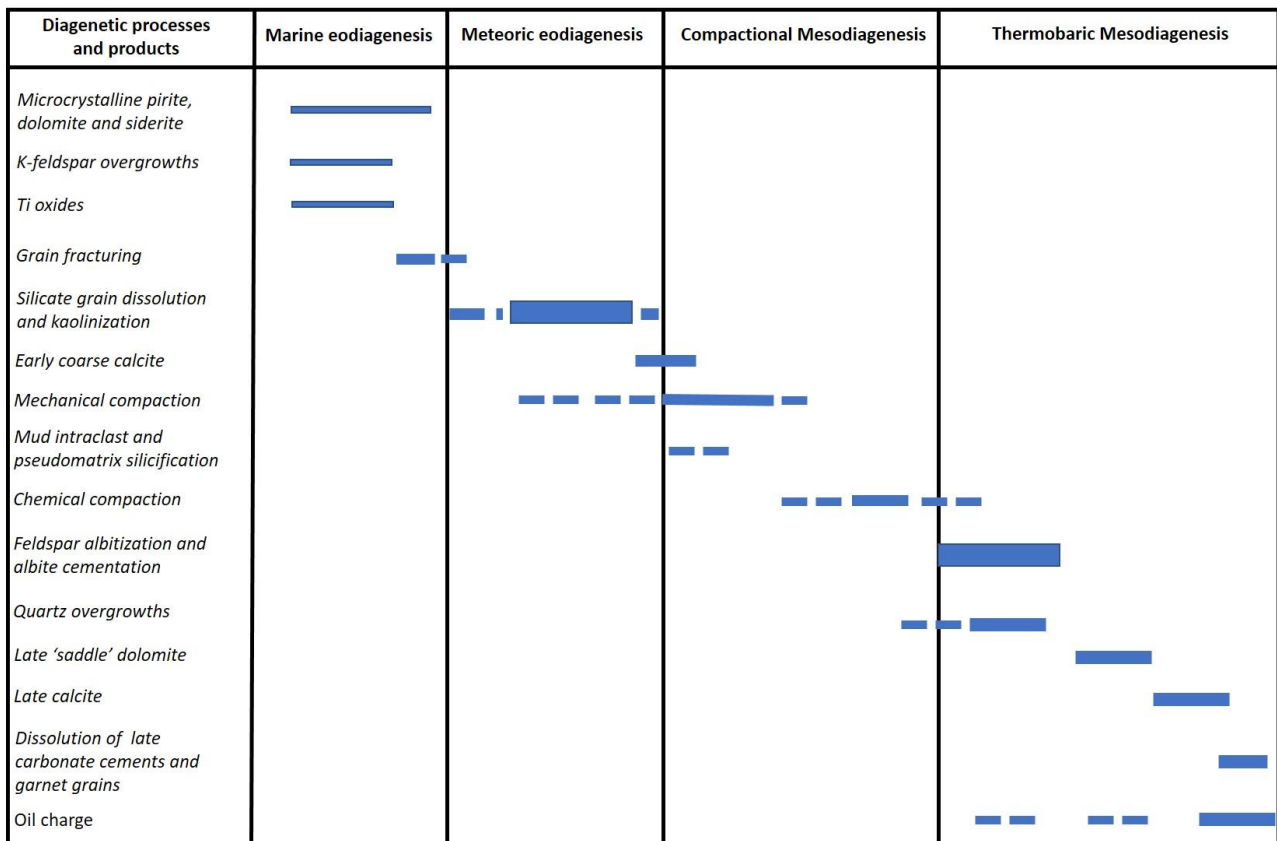| Diagenetic processes and products	Marine eodiagenesis	Meteoric eodiagenesis	Compactional Mesodiagenesis	Thermobaric Mesodiagenesis
Microcrystalline pirite, dolomite and siderite	▬			
K-feldspar overgrowths	▬			
Ti oxides	▬			
Grain fracturing	▬			
Silicate grain dissolution and kaolinization		▬▬		
Early coarse calcite			▬	
Mechanical compaction		▬ ▬ ▬	▬▬	
Mud intraclast and pseudomatrix silicification			▬ ▬	
Chemical compaction			▬ ▬ ▬	▬
Feldspar albitization and albite cementation				▬▬
Quartz overgrowths			▬	▬
Late 'saddle' dolomite				▬
Late calcite				▬
Dissolution of late carbonate cements and garnet grains				▬
Oil charge			▬ ▬ ▬ ▬	▬▬

Figure 10. Mineral paragenesis in the Urucutuca Sandstones from the Cangoá and Peroá Fields. Relative thickness of the bars reflects the significance of each diagenetic process/product. The definition of diagenetic stages incorporates the concept of hidrogeologic regimes proposed by Galloway (1984).
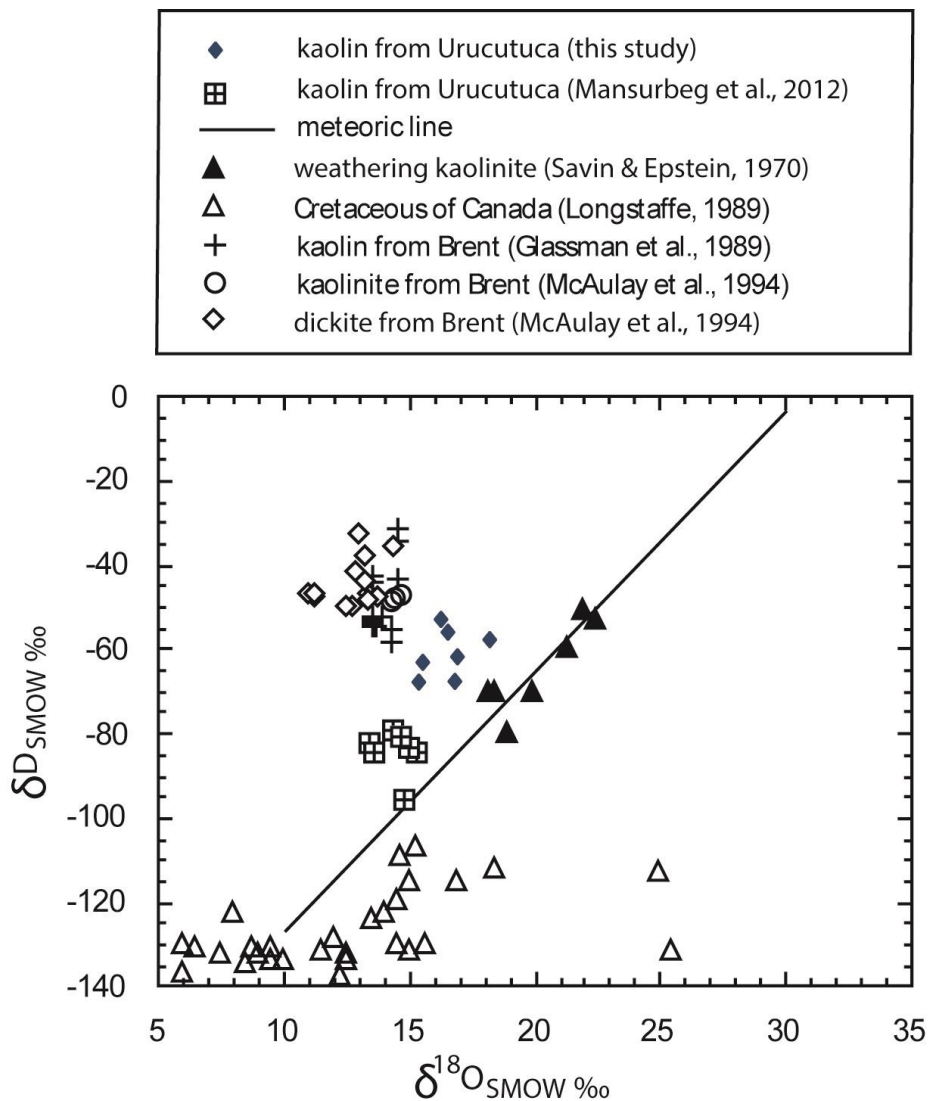
Figure 11. Plot of $\delta^{18}O_{VSMOW}$ versus δD_{VSMOW} values of diagenetic kaolin from different sandstones and weathering kaolinites. Kaolinites from the Urucutuca sandstones are situated close to the line of meteoric kaolinites.
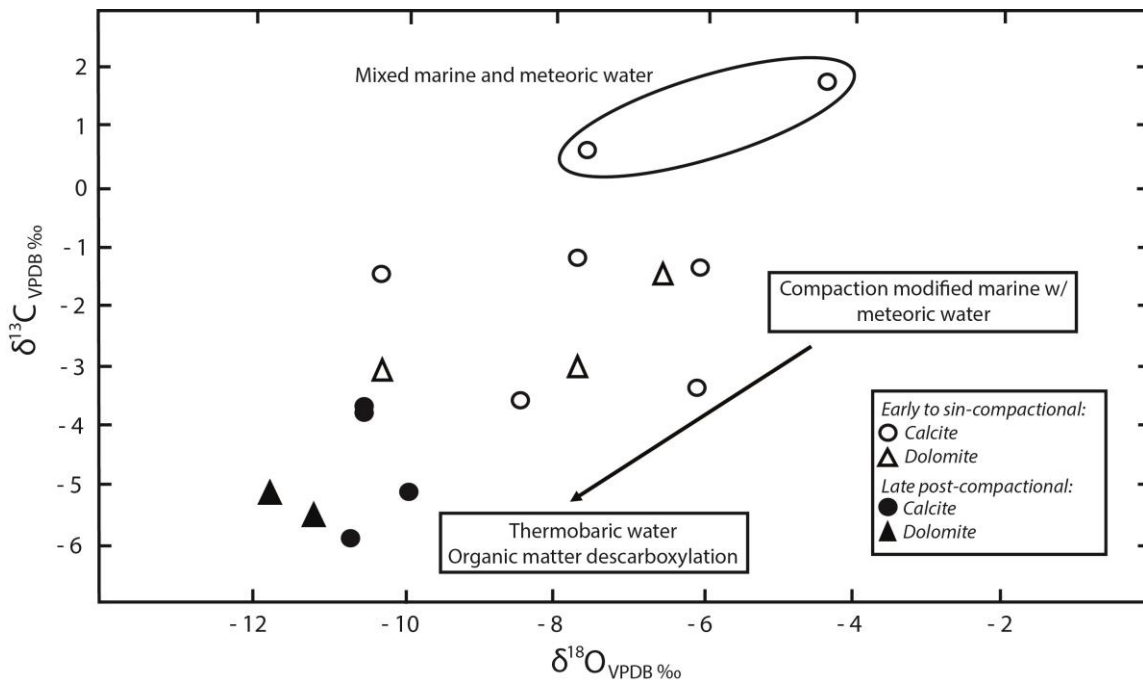
Figure 12. Carbon and oxygen stable isotope cross plot for authigenic calcite and dolomite. Note a clear covariance trend from early towards late phases which indicates a progressive contribution of evolved fluids and the influence of organic matter descarboxylation due to thermal maturation and compaction.

Figure 13. Total diagenetic albite and Total albite/Total feldspar ratio plotted against each well and their relative distance from the salt dome for Cangoá (A) and Peroá (B).

Table 1: Major present and original constituents of the studied sandstones.

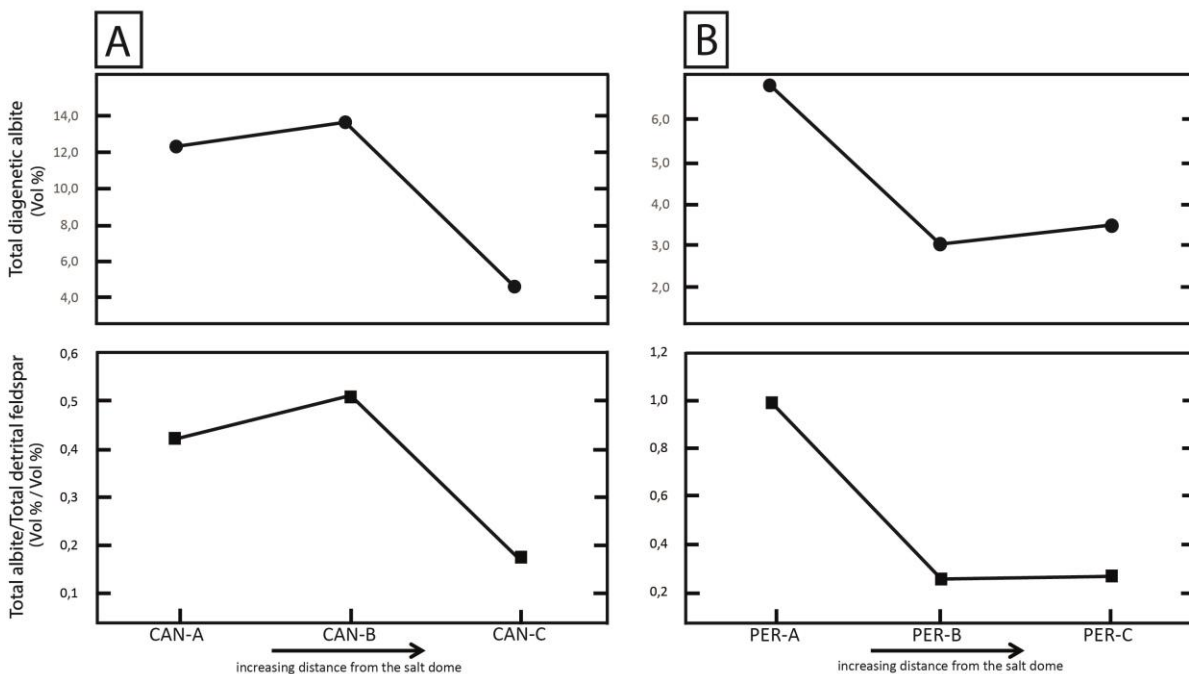| Well	CAN-A	CAN-B	CAN-C	PER-A	PER-B	PER-C	Min.	Max.	Average
Number of samples	(23)	(7)	(17)	(17)	(13)	(8)			
Present detrital minerals									
Total detrital quartz	**39,6**	**40**	**41,9**	**49**	**38,3**	**32,3**	**32,3**	**49,0**	**40,2**
Quartz monocrystalline	39	37,7	40	48,3	37,4	31,5	**31,5**	**48,3**	**39,0**
Quartz polycrystalline	0,5	2,3	1,9	0,7	0,9	0,8	**0,5**	**2,3**	**1,2**
Total detrital feldspar	**13**	**9,6**	**20,1**	**10,3**	**19**	**11,6**	**9,6**	**20,1**	**13,9**
K-feldspar	3,2	5,3	6,8	5,6	7,7	6,9	**3,2**	**7,7**	**5,9**
Orthoclase	1,5	1,1	1,5	0,1	1,2	1,7	**0,1**	**1,7**	**1,2**
Microcline	1,2	2,4	4,4	4	5,7	3,7	**1,2**	**5,7**	**3,6**
Perthite	0,4	1,8	0,7	1,1	0,4	1,2	**0,4**	**1,8**	**0,9**
Total Plagioclase	**9,8**	**4,2**	**13,3**	**4,7**	**11,2**	**4,7**	**4,2**	**13,3**	**8,0**
Untwinned plagioclase	8,3	3,3	7,2	4	8,5	2,3	**2,3**	**8,5**	**5,6**
Twinned plagioclase	1	0,9	5,9	0,5	2,6	1,8	**0,5**	**5,9**	**2,1**
Plutonic lithic fragments	3,3	1,8	2	1,4	0,8	3,4	**0,8**	**3,4**	**2,1**
Micas	1,1	0,6	1,1	0,4	0,8	1,4	**0,4**	**1,4**	**0,9**
Garnet	0,1	0,4	0,4	0,1	0,2	0,8	**0,1**	**0,8**	**0,3**
Other heavy minerals	0,2	0,5	0,6	0,3	0,3	0,6	**0,2**	**0,6**	**0,4**
Carbonate grains	0,7	0,3	1,6	0,7	1,4	2,8	**0,3**	**2,8**	**1,3**
Diagenetic Minerals									
Quartz intergranular	3,4	2,6	1,8	0,4	0,1	0,9	**0,1**	**3,4**	**1,5**
Albite intergranular	2,2	1,1	0,5	0,1	0,6	0,3	**0,1**	**2,2**	**0,8**
Albite intragranular	10,1	12,6	4,1	6,8	2,5	4,2	**2,5**	**12,6**	**6,7**
Calcite intergranular	6	0,8	8,7	14,8	8,4	7,5	**0,8**	**14,8**	**7,7**
Calcite intragranular	8,3	3,3	2,9	3,8	8,4	12,9	**2,9**	**12,9**	**6,6**
Dolomite intergranular	3,7	0,7	0,4	0,4	0,4	0,5	**0,4**	**3,7**	**1,0**
Dolomite intragranular	2	3,6	0,7	0,2	0,6	1,2	**0,2**	**3,6**	**1,4**
Kaolinite intergranular	0,1	1	0,4	0,4	0,8	2,9	**0,1**	**2,9**	**0,9**
Kaolinite intragranular	2,1	3,4	2,3	2,1	2,6	4,7	**2,1**	**4,7**	**2,9**
Total macroporosity	**4,2**	**10,3**	**5,9**	**9,3**	**8,1**	**8,7**	**4,2**	**10,3**	**7,8**
Intergranular macroporosity	2,3	6,4	4,1	7,3	5,7	4	**2,3**	**7,3**	**5,0**
Intragranular macroporosity	1,9	3,9	1,8	2	2,4	4,7	**1,8**	**4,7**	**2,8**
Original detrital constituents									
Original detrital quartz	34,2	40	37,1	38,1	36,3	31,5	**31,5**	**40,0**	**36,2**
Original detrital K-feldspars	6,5	11,1	9,4	7,8	9	18,9	**6,5**	**18,9**	**10,5**
Original detrital plagioclase	22,6	15,5	18,2	6,9	12,1	13,4	**6,9**	**22,6**	**14,8**
Original micas	2,9	1,5	2,6	0,8	2,4	6,7	**0,8**	**6,7**	**2,8**
Original carbonate grains	0,6	0,5	1,7	0,7	1,3	3,5	**0,5**	**3,5**	**1,4**
Original intergranular porosity	**36**	**34,1**	**31,9**	**35,8**	**34**	**25,9**	**25,9**	**36,0**	**33,0**

Table 2 - Results of stable isotopes analyses of diagenetic carbonates in the studied sandstones.

Sample Number	Description	$\delta^{13}C_{VPDB}$ (‰)	$^{18}O_{VSMOW}$ (‰)	$\delta^{18}O_{VPDB}$ (‰)
PER-C-ESS 2663.9 #5	Early calcite	1.76	26.48	-4.30
PER-A-ES 2814.75 #1	Early calcite	-3.59	22.25	-8.40
PER-A-ES 3013.1 #3	Sin-compactional Fe-calcite	0.62	23.17	-7.51
PER-A-ES 3265.7 #4	Sin-compactional Fe-calcite	-1.48	20.36	-10.23
PER-B-ES 2756.4 #3	Early Fe-calcite	-1.18	23.05	-7.62
PER-B-ES 2750.10 #3	Early Fe-calcite	-3.36	24.69	-6.03
CAN-C-ES 3079.50 #1	Early calcite (locally corrosive)	-1.33	24.71	-6.01
CAN-A-ES 3162.05 #1	Late calcite (after dolomite)	-3.70	20.13	-10.46
CAN-A-ES 3312.2 #2	Late calcite (corrosive)	-5.13	20.74	-9.86
CAN-A-ES 3313.70 #2	Late Fe-calcite (after dolomite)	-5.90	19.92	-10.66
CAN-C-ES 3078.85 #1	Late calcite	-3.76	20.11	-10.47
CAN-C-ES 3079.50 #1	Fe-dolomite (saddle)	-1.43	24.21	-6.50
CAN-C-ES 3088.35 #1	Fe-dolomite (replacive)	-3,07	20.34	-10,24
CAN-A-ES 3162.65 #1	Sin-compactional dolomite (saddle)	-3,00	23,04	-7,63
CAN-A-ES 3317.2 #2	Late blocky dolomite	-5.13	18.82	-11.72
CAN-A-ES 3312.2 #2	Late Fe-dolomite (saddle)	-5.48	19.41	-11.15

Table 3 – Summary of the microthermometry analyses of quartz fluid inclusions

Sample Depth	Occurrence	Th HC (°C)	Th aq (°C)	Sal (wt%)
PER-A				
2905 m	dust rim and overgrowth		100 - 119	8 - 10.6
CAN-A				
3312.5 m	dust rim and overgrowth	130	125 - 155	9.6 - 13.6
3317.9 m			130 - 145	11.9 - 4.3
CAN-C				
3087.4 m	dust rim, ingrowth in grain fracture and overgrowth	115 - 135	110 - 135	10.1 - 16
3092.25 m		120 - 145	115 - 146	9.2 - 10.0

Th HC (°C): homogenization temperature of petroleum inclusions

TH aq (°C): homogenization temperature of aqueous inclusions

Sal (wt%): salinity computed from NaCl-H2O system